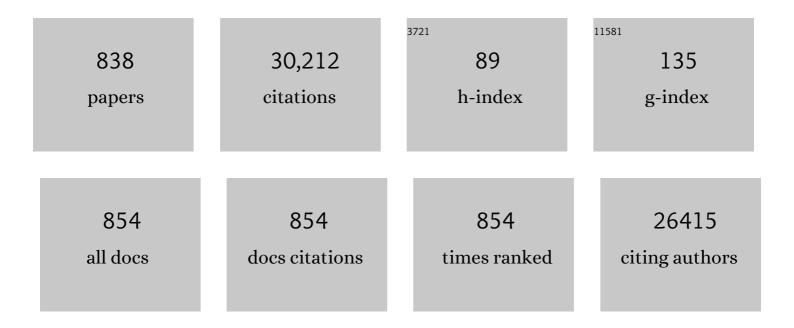
Joan R Morante

List of Publications by Year in descending order

Source: https://exaly.com/author-pdf/4780388/publications.pdf Version: 2024-02-01



#	Article	IF	CITATIONS
1	The complete Raman spectrum of nanometric SnO2 particles. Journal of Applied Physics, 2001, 90, 1550-1557.	1.1	686
2	Structural and optical properties of high quality zinc-blende/wurtzite GaAs nanowire heterostructures. Physical Review B, 2009, 80, .	1.1	434
3	Recent developments in organic redox flow batteries: A critical review. Journal of Power Sources, 2017, 360, 243-283.	4.0	396
4	Self-assembled quantum dots in a nanowire system for quantum photonics. Nature Materials, 2013, 12, 439-444.	13.3	306
5	Effects of Nb doping on the TiO2 anatase-to-rutile phase transition. Journal of Applied Physics, 2002, 92, 853-861.	1.1	301
6	In-depth resolved Raman scattering analysis for the identification of secondary phases: Characterization of Cu2ZnSnS4 layers for solar cell applications. Applied Physics Letters, 2011, 98, .	1.5	287
7	Analysis of the noble metal catalytic additives introduced by impregnation of as obtained SnO2 sol–gel nanocrystals for gas sensors. Sensors and Actuators B: Chemical, 2000, 70, 87-100.	4.0	286
8	Nucleation mechanism of gallium-assisted molecular beam epitaxy growth of gallium arsenide nanowires. Applied Physics Letters, 2008, 92, .	1.5	261
9	Influence of average size and interface passivation on the spectral emission of Si nanocrystals embedded in SiO2. Journal of Applied Physics, 2002, 91, 798-807.	1.1	259
10	Cr-doped TiO2 gas sensor for exhaust NO2 monitoring. Sensors and Actuators B: Chemical, 2003, 93, 509-518.	4.0	241
11	Synthesis and Characterization of Chromium-Doped Mesoporous Tungsten Oxide for Gas Sensing Applications. Advanced Functional Materials, 2007, 17, 1801-1806.	7.8	241
12	Review of zinc-based hybrid flow batteries: From fundamentals to applications. Materials Today Energy, 2018, 8, 80-108.	2.5	224
13	Raman spectroscopy of wurtzite and zinc-blende GaAs nanowires: Polarization dependence, selection rules, and strain effects. Physical Review B, 2009, 80, .	1.1	222
14	High mobility indium free amorphous oxide thin film transistors. Applied Physics Letters, 2008, 92, .	1.5	210
15	Bi2O3 as a selective sensing material for NO detection. Sensors and Actuators B: Chemical, 2004, 99, 74-89.	4.0	206
16	Vibrational properties of stannite and kesterite type compounds: Raman scattering analysis of Cu2(Fe,Zn)SnS4. Journal of Alloys and Compounds, 2012, 539, 190-194.	2.8	201
17	Cu ₂ ZnGeSe ₄ Nanocrystals: Synthesis and Thermoelectric Properties. Journal of the American Chemical Society, 2012, 134, 4060-4063.	6.6	199
18	Crystalline structure, defects and gas sensor response to NO2 and H2S of tungsten trioxide nanopowders. Sensors and Actuators B: Chemical, 2003, 93, 475-485.	4.0	196

#	Article	IF	CITATIONS
19	Morphological analysis of nanocrystalline SnO2 for gas sensor applications. Sensors and Actuators B: Chemical, 1996, 31, 1-8.	4.0	195
20	Equivalence between thermal and room temperature UV light-modulated responses of gas sensors based on individual SnO2 nanowires. Sensors and Actuators B: Chemical, 2009, 140, 337-341.	4.0	195
21	Direct correlation of crystal structure and optical properties in wurtzite/zinc-blende GaAs nanowire heterostructures. Physical Review B, 2011, 83, .	1.1	193
22	Slightly hydrogenated TiO ₂ with enhanced photocatalytic performance. Journal of Materials Chemistry A, 2014, 2, 12708-12716.	5.2	188
23	Gallium–Indium–Zinc-Oxide-Based Thin-Film Transistors: Influence of the Source/Drain Material. IEEE Transactions on Electron Devices, 2008, 55, 954-960.	1.6	185
24	Enhanced photoelectrochemical water splitting of hematite multilayer nanowire photoanodes by tuning the surface state via bottom-up interfacial engineering. Energy and Environmental Science, 2017, 10, 2124-2136.	15.6	185
25	Ultralow power consumption gas sensors based on self-heated individual nanowires. Applied Physics Letters, 2008, 93, .	1.5	184
26	Insights into the Structural and Chemical Modifications of Nb Additive on TiO2 Nanoparticles. Chemistry of Materials, 2004, 16, 862-871.	3.2	182
27	The Role of Surface Oxygen Vacancies in the NO ₂ Sensing Properties of SnO ₂ Nanocrystals. Journal of Physical Chemistry C, 2008, 112, 19540-19546.	1.5	181
28	Nanostructured metal oxides synthesized by hard template method for gas sensing applications. Sensors and Actuators B: Chemical, 2005, 109, 57-63.	4.0	176
29	The effects of electron–hole separation on the photoconductivity of individual metal oxide nanowires. Nanotechnology, 2008, 19, 465501.	1.3	169
30	Mesoporous WO3 photocatalyst for the partial oxidation of methane to methanol using electron scavengers. Applied Catalysis B: Environmental, 2015, 163, 150-155.	10.8	166
31	High response and stability in CO and humidity measures using a single SnO2 nanowire. Sensors and Actuators B: Chemical, 2007, 121, 3-17.	4.0	165
32	Influence of the catalytic introduction procedure on the nano-SnO2 gas sensor performances. Sensors and Actuators B: Chemical, 2001, 79, 98-106.	4.0	162
33	Raman Surface Vibration Modes in Nanocrystalline SnO2:  Correlation with Gas Sensor Performances. Chemistry of Materials, 2005, 17, 893-901.	3.2	162
34	Photoelectrochemical water splitting: a road from stable metal oxides to protected thin film solar cells. Journal of Materials Chemistry A, 2020, 8, 10625-10669.	5.2	162
35	Polarity Assignment in ZnTe, GaAs, ZnO, and GaN-AlN Nanowires from Direct Dumbbell Analysis. Nano Letters, 2012, 12, 2579-2586.	4.5	161
36	Analysis of buried etch-stop layers in silicon by nitrogen-ion implantation. Journal of Micromechanics and Microengineering, 1993, 3, 143-145.	1.5	160

Joan R Morante

#	Article	IF	CITATIONS
37	The influence of film structure on In2O3 gas response. Thin Solid Films, 2004, 460, 315-323.	0.8	155
38	Synthesis of Silicon Nanowires with Wurtzite Crystalline Structure by Using Standard Chemical Vapor Deposition. Advanced Materials, 2007, 19, 1347-1351.	11.1	155
39	Composition Control and Thermoelectric Properties of Quaternary Chalcogenide Nanocrystals: The Case of Stannite Cu ₂ CdSnSe ₄ . Chemistry of Materials, 2012, 24, 562-570.	3.2	153
40	Combined High Catalytic Activity and Efficient Polar Tubular Nanostructure in Urchin‣ike Metallic NiCo ₂ Se ₄ for Highâ€Performance Lithium–Sulfur Batteries. Advanced Functional Materials, 2019, 29, 1903842.	7.8	153
41	Engineering grain boundaries at theÂ2D limit for theÂhydrogen evolution reaction. Nature Communications, 2020, 11, 57.	5.8	153
42	Heterostructured p-CuO (nanoparticle)/n-SnO2 (nanowire) devices for selective H2S detection. Sensors and Actuators B: Chemical, 2013, 181, 130-135.	4.0	148
43	From rational design of a new bimetallic MOF family with tunable linkers to OER catalysts. Journal of Materials Chemistry A, 2019, 7, 1616-1628.	5.2	148
44	What do you do, titanium? Insight into the role of titanium oxide as a water oxidation promoter in hematite-based photoanodes. Energy and Environmental Science, 2015, 8, 3242-3254.	15.6	147
45	Influence of Cu as a catalyst on the properties of silicon nanowires synthesized by the vapour–solid–solid mechanism. Nanotechnology, 2007, 18, 305606.	1.3	144
46	Prismatic Quantum Heterostructures Synthesized on Molecularâ€Beam Epitaxy GaAs Nanowires. Small, 2008, 4, 899-903.	5.2	142
47	Size dependence of lifetime and absorption cross section of Si nanocrystals embedded in SiO2. Applied Physics Letters, 2003, 82, 1595-1597.	1.5	139
48	Perovskite-type BaSnO3 powders for high temperature gas sensor applications. Sensors and Actuators B: Chemical, 2002, 84, 21-25.	4.0	138
49	Structural stability of indium oxide films deposited by spray pyrolysis during thermal annealing. Thin Solid Films, 2005, 479, 38-51.	0.8	137
50	Core–Shell Nanoparticles As Building Blocks for the Bottom-Up Production of Functional Nanocomposites: PbTe–PbS Thermoelectric Properties. ACS Nano, 2013, 7, 2573-2586.	7.3	137
51	Nucleation and growth of GaN nanorods on Si (111) surfaces by plasma-assisted molecular beam epitaxy - The influence of Si- and Mg-doping. Journal of Applied Physics, 2008, 104, .	1.1	136
52	Raman scattering and disorder effect in Cu ₂ ZnSnS ₄ . Physica Status Solidi - Rapid Research Letters, 2013, 7, 258-261.	1.2	136
53	Fabrication and electrical characterization of circuits based on individual tin oxide nanowires. Nanotechnology, 2006, 17, 5577-5583.	1.3	135
54	GdBaCo2O5+x layered perovskite as an intermediate temperature solid oxide fuel cell cathode. Journal of Power Sources, 2007, 174, 255-263.	4.0	135

#	Article	lF	CITATIONS
55	Role of Tungsten Doping on the Surface States in BiVO ₄ Photoanodes for Water Oxidation: Tuning the Electron Trapping Process. ACS Catalysis, 2018, 8, 3331-3342.	5.5	135
56	Role of Ga2O3–In2O3–ZnO channel composition on the electrical performance of thin-film transistors. Materials Chemistry and Physics, 2011, 131, 512-518.	2.0	134
57	Influence of surface Pd doping on gas sensing characteristics of SnO2 thin films deposited by spray pirolysis. Thin Solid Films, 2003, 436, 119-126.	0.8	133
58	Toward a Systematic Understanding of Photodetectors Based on Individual Metal Oxide Nanowires. Journal of Physical Chemistry C, 2008, 112, 14639-14644.	1.5	130
59	A Novel Mesoporous CaOâ€Loaded In ₂ O ₃ Material for CO ₂ Sensing. Advanced Functional Materials, 2007, 17, 2957-2963.	7.8	129
60	Partial Oxidation of Methane to Methanol Using Bismuth-Based Photocatalysts. ACS Catalysis, 2014, 4, 3013-3019.	5.5	127
61	Tubular CoFeP@CN as a Mott–Schottky Catalyst with Multiple Adsorption Sites for Robust Lithiumâ~'Sulfur Batteries. Advanced Energy Materials, 2021, 11, 2100432.	10.2	125
62	Micromachined twin gas sensor for CO and O2 quantification based on catalytically modified nano-SnO2. Sensors and Actuators B: Chemical, 2006, 114, 881-892.	4.0	124
63	Active nano-CuPt3 electrocatalyst supported on graphene for enhancing reactions at the cathode in all-vanadium redox flow batteries. Carbon, 2012, 50, 2372-2374.	5.4	124
64	Three-Dimensional Multiple-Order Twinning of Self-Catalyzed GaAs Nanowires on Si Substrates. Nano Letters, 2011, 11, 3827-3832.	4.5	123
65	Elucidation of the surface passivation role on the photoluminescence emission yield of silicon nanocrystals embedded in SiO2. Applied Physics Letters, 2002, 80, 1637-1639.	1.5	117
66	In2O3 films deposited by spray pyrolysis as a material for ozone gas sensors. Sensors and Actuators B: Chemical, 2004, 99, 297-303.	4.0	117
67	Correlation between XPS, Raman and TEM measurements and the gas sensitivity of Pt and Pd doped SnO 2 based gas sensors. Fresenius' Journal of Analytical Chemistry, 1998, 361, 110-114.	1.5	116
68	An insight on the role of La in mesoporous WO 3 for the photocatalytic conversion of methane into methanol. Applied Catalysis B: Environmental, 2016, 187, 30-36.	10.8	116
69	A prototype reactor for highly selective solar-driven CO ₂ reduction to synthesis gas using nanosized earth-abundant catalysts and silicon photovoltaics. Energy and Environmental Science, 2017, 10, 2256-2266.	15.6	116
70	Use of zeolite films to improve the selectivity of reactive gas sensors. Catalysis Today, 2003, 82, 179-185.	2.2	114
71	ZnSe/N-Doped Carbon Nanoreactor with Multiple Adsorption Sites for Stable Lithium–Sulfur Batteries. ACS Nano, 2020, 14, 15492-15504.	7.3	114
72	Strategies for enhancing electrochemical activity of carbon-based electrodes for all-vanadium redox flow batteries. Applied Energy, 2013, 109, 344-351.	5.1	112

#	Article	IF	CITATIONS
73	Metal Ions To Control the Morphology of Semiconductor Nanoparticles: Copper Selenide Nanocubes. Journal of the American Chemical Society, 2013, 135, 4664-4667.	6.6	112
74	Thermal and mechanical analysis of micromachined gas sensors. Journal of Micromechanics and Microengineering, 2003, 13, 548-556.	1.5	111
75	Morphology evolution of Cu2â^xS nanoparticles: from spheres to dodecahedrons. Chemical Communications, 2011, 47, 10332.	2.2	107
76	Thermo–chemical treatments based on NH3/O2 for improved graphite-based fiber electrodes in vanadium redox flow batteries. Carbon, 2013, 60, 280-288.	5.4	107
77	Effects of various metal additives on the gas sensing performances of TiO2 nanocrystals obtained from hydrothermal treatments. Sensors and Actuators B: Chemical, 2005, 108, 34-40.	4.0	106
78	Electrical properties of individual tin oxide nanowires contacted to platinum electrodes. Physical Review B, 2007, 76, .	1.1	105
79	Synergistic effects in 3D honeycomb-like hematite nanoflakes/branched polypyrrole nanoleaves heterostructures as high-performance negative electrodes for asymmetric supercapacitors. Nano Energy, 2016, 22, 189-201.	8.2	102
80	NH3interaction with chromium-doped WO3nanocrystalline powders for gas sensing applications. Journal of Materials Chemistry, 2004, 14, 2412-2420.	6.7	100
81	InAs Quantum Dot Arrays Decorating the Facets of GaAs Nanowires. ACS Nano, 2010, 4, 5985-5993.	7.3	99
82	p-GaN/n-ZnO Heterojunction Nanowires: Optoelectronic Properties and the Role of Interface Polarity. ACS Nano, 2014, 8, 4376-4384.	7.3	99
83	Microstructure control of thermally stable TiO2 obtained by hydrothermal process for gas sensors. Sensors and Actuators B: Chemical, 2004, 103, 312-317.	4.0	98
84	Nanoparticle engineering for gas sensor optimisation: improved sol–gel fabricated nanocrystalline SnO2 thick film gas sensor for NO2 detection by calcination, catalytic metal introduction and grinding treatments. Sensors and Actuators B: Chemical, 1999, 60, 125-137.	4.0	97
85	Nanocrystalline Metal Oxides from the Injection of Metal Oxide Sols in Coordinating Solutions: Synthesis, Characterization, Thermal Stabilization, Device Processing, and Gas-Sensing Properties. Advanced Functional Materials, 2006, 16, 1488-1498.	7.8	97
86	Insight into the Role of Oxygen Diffusion in the Sensing Mechanisms of SnO ₂ Nanowires. Advanced Functional Materials, 2008, 18, 2990-2994.	7.8	96
87	Synthesis of perovskite-type BaSnO3 particles obtained by a new simple wet chemical route based on a sol–gel process. Materials Letters, 2002, 56, 131-136.	1.3	95
88	Experimental and theoretical studies of indium oxide gas sensors fabricated by spray pyrolysis. Sensors and Actuators B: Chemical, 2005, 106, 563-571.	4.0	94
89	Defect study of SnO2 nanostructures by cathodoluminescence analysis: Application to nanowires. Sensors and Actuators B: Chemical, 2007, 126, 6-12.	4.0	93
90	Mesoporous catalytic filters for semiconductor gas sensors. Thin Solid Films, 2003, 436, 64-69.	0.8	91

#	Article	IF	CITATIONS
91	Atomically dispersed Fe in a C ₂ N Based Catalyst as a Sulfur Host for Efficient Lithium–Sulfur Batteries. Advanced Energy Materials, 2021, 11, 2003507.	10.2	91
92	Charge Exchange Processes during the Open-Circuit Deposition of Nickel on Silicon from Fluoride Solutions. Journal of the Electrochemical Society, 2000, 147, 1026.	1.3	90
93	Synthesis and electrochemical properties of 2D molybdenum vanadium carbides – solid solution MXenes. Journal of Materials Chemistry A, 2020, 8, 8957-8968.	5.2	90
94	The aging effect on SnO2–Au thin film sensors: electrical and structural characterization. Thin Solid Films, 2000, 371, 249-253.	0.8	89
95	Correlation between structural and optical properties of Si nanocrystals embedded in SiO2: The mechanism of visible light emission. Applied Physics Letters, 2000, 77, 3143-3145.	1.5	89
96	A new CO2 gas sensing material. Sensors and Actuators B: Chemical, 2003, 95, 266-270.	4.0	89
97	Controlled Photocatalytic Oxidation of Methane to Methanol through Surface Modification of Beta Zeolites. ACS Catalysis, 2017, 7, 2878-2885.	5.5	89
98	NbSe ₂ Meets C ₂ N: A 2Dâ€2D Heterostructure Catalysts as Multifunctional Polysulfide Mediator in Ultra‣ong‣ife Lithium–Sulfur Batteries. Advanced Energy Materials, 2021, 11, 2101250.	10.2	89
99	Long range epitaxial growth of prismatic heterostructures on the facets of catalyst-free GaAs nanowires. Journal of Materials Chemistry, 2009, 19, 840.	6.7	88
100	Economic viability of SNG production from power and CO2. Energy Conversion and Management, 2018, 162, 218-224.	4.4	88
101	Strategies to enhance the carbon monoxide sensitivity of tin oxide thin films. Sensors and Actuators B: Chemical, 2003, 95, 90-96.	4.0	87
102	Vibrational and crystalline properties of polymorphicCuInC2(C=Se,S)chalcogenides. Physical Review B, 2005, 71, .	1.1	86
103	Ab initio study of NOx compounds adsorption on SnO2 surface. Sensors and Actuators B: Chemical, 2007, 126, 62-67.	4.0	86
104	Influence of the (111) twinning on the formation of diamond cubic/diamond hexagonal heterostructures in Cu-catalyzed Si nanowires. Journal of Applied Physics, 2008, 104, .	1.1	86
105	Colloidal synthesis and thermoelectric properties of Cu ₂ SnSe ₃ nanocrystals. Journal of Materials Chemistry A, 2013, 1, 1421-1426.	5.2	86
106	A High Conductivity 1D π–d Conjugated Metal–Organic Framework with Efficient Polysulfide Trappingâ€Diffusion atalysis in Lithium–Sulfur Batteries. Advanced Materials, 2022, 34, e2108835.	11.1	86
107	Study of the CO and humidity interference in La doped tin oxide CO2 gas sensor. Sensors and Actuators B: Chemical, 2003, 94, 324-329.	4.0	84
108	Triple-twin domains in Mg doped GaN wurtzite nanowires: structural and electronic properties of this zinc-blende-like stacking. Nanotechnology, 2009, 20, 145704.	1.3	84

#	Article	IF	CITATIONS
109	Ultrasensitive binder-free glucose sensors based on the pyrolysis of in situ grown Cu MOF. Sensors and Actuators B: Chemical, 2018, 254, 272-281.	4.0	84
110	Insight on the SU-8 resist as passivation layer for transparent Ga2O3–In2O3–ZnO thin-film transistors. Journal of Applied Physics, 2010, 108, .	1.1	83
111	MoS <i>_x</i> @NiO Composite Nanostructures: An Advanced Nonprecious Catalyst for Hydrogen Evolution Reaction in Alkaline Media. Advanced Functional Materials, 2019, 29, 1807562.	7.8	83
112	Surface activation by Pt-nanoclusters on titania for gas sensing applications. Materials Science and Engineering C, 2002, 19, 105-109.	3.8	82
113	High-temperature low-power performing micromachined suspended micro-hotplate for gas sensing applications. Sensors and Actuators B: Chemical, 2006, 114, 826-835.	4.0	81
114	Analysis of the catalytic activity and electrical characteristics of different modified SnO2 layers for gas sensors. Sensors and Actuators B: Chemical, 2002, 84, 12-20.	4.0	79
115	Crystallographic Control at the Nanoscale To Enhance Functionality: Polytypic Cu ₂ GeSe ₃ Nanoparticles as Thermoelectric Materials. Chemistry of Materials, 2012, 24, 4615-4622.	3.2	79
116	Solvothermal, Chloroalkoxide-based Synthesis of Monoclinic WO ₃ Quantum Dots and Gas-Sensing Enhancement by Surface Oxygen Vacancies. ACS Applied Materials & Interfaces, 2014, 6, 16808-16816.	4.0	78
117	Stable high-voltage aqueous pseudocapacitive energy storage device with slow self-discharge. Nano Energy, 2019, 64, 103961.	8.2	78
118	Influence on the gas sensor performances of the metal chemical states introduced by impregnation of calcinated SnO2 sol–gel nanocrystals. Sensors and Actuators B: Chemical, 2000, 68, 94-99.	4.0	77
119	MicroRaman scattering from polycrystalline CuInS 2 films: structural analysis. Thin Solid Films, 2000, 361-362, 208-212.	0.8	77
120	On the role of individual metal oxide nanowires in the scaling down of chemical sensors. Physical Chemistry Chemical Physics, 2009, 11, 7105.	1.3	77
121	Measurement of residual stress by slot milling with focused ion-beam equipment. Journal of Micromechanics and Microengineering, 2006, 16, 254-259.	1.5	76
122	Ab initio calculations of NO2 and SO2 chemisorption onto non-polar ZnO surfaces. Sensors and Actuators B: Chemical, 2009, 142, 179-184.	4.0	76
123	Synthesis of nanocrystalline materials for SOFC applications by acrylamide polymerisation. Journal of Power Sources, 2003, 118, 256-264.	4.0	75
124	Polymorphism in CuInS2 epilayers: Origin of additional Raman modes. Applied Physics Letters, 2002, 80, 562-564.	1.5	74
125	White luminescence from Si+ and C+ ion-implanted SiO2 films. Journal of Applied Physics, 2003, 94, 254-262.	1.1	74
126	Influence of Cu-, Fe-, Co-, and Mn-oxide nanoclusters on sensing behavior of SnO2 films. Thin Solid Films, 2004, 467, 209-214.	0.8	73

#	Article	IF	CITATIONS
127	In2O3 films deposited by spray pyrolysis: gas response to reducing (CO, H2) gases. Sensors and Actuators B: Chemical, 2004, 98, 122-129.	4.0	73
128	Suppression of three dimensional twinning for a 100% yield of vertical GaAs nanowires on silicon. Nanoscale, 2012, 4, 1486.	2.8	73
129	Self-Assembled GaN Nanowires on Diamond. Nano Letters, 2012, 12, 2199-2204.	4.5	73
130	Selective anodes for seawater splitting via functionalization of manganese oxides by a plasma-assisted process. Applied Catalysis B: Environmental, 2021, 284, 119684.	10.8	73
131	Improvement of oxygen storage capacity using mesoporous ceria–zirconia solid solutions. Applied Catalysis B: Environmental, 2011, 108-109, 32-38.	10.8	72
132	Efficient WO3 photoanodes fabricated by pulsed laser deposition for photoelectrochemical water splitting with high faradaic efficiency. Applied Catalysis B: Environmental, 2016, 189, 133-140.	10.8	72
133	Improved selectivity for partial oxidation of methane to methanol in the presence of nitrite ions and BiVO ₄ photocatalyst. Chemical Communications, 2015, 51, 7249-7252.	2.2	71
134	Optimization of tin dioxide nanosticks faceting for the improvement of palladium nanocluster epitaxy. Applied Physics Letters, 2002, 80, 329-331.	1.5	70
135	Catalyst-free nanowires with axial In _{<i>x</i>} Ga _{1â~°<i>x</i>} As <i>/</i> GaAs heterostructures. Nanotechnology, 2009, 20, 075603.	1.3	70
136	Tailor-made metal-nitrogen-carbon bifunctional electrocatalysts for rechargeable Zn-air batteries via controllable MOF units. Energy Storage Materials, 2019, 17, 46-61.	9.5	70
137	Synthesis and Gas-Sensing Properties of Pd-Doped SnO ₂ Nanocrystals. A Case Study of a General Methodology for Doping Metal Oxide Nanocrystals. Crystal Growth and Design, 2008, 8, 1774-1778.	1.4	69
138	Site of Er ions in silica layers codoped with Si nanoclusters and Er. Applied Physics Letters, 2006, 88, 121915.	1.5	68
139	Portable microsensors based on individual SnO ₂ nanowires. Nanotechnology, 2007, 18, 495501.	1.3	68
140	Gallium assisted plasma enhanced chemical vapor deposition of silicon nanowires. Nanotechnology, 2009, 20, 155602.	1.3	68
141	Electrospun Black Titania Nanofibers: Influence of Hydrogen Plasma-Induced Disorder on the Electronic Structure and Photoelectrochemical Performance. Journal of Physical Chemistry C, 2015, 119, 18835-18842.	1.5	68
142	Optical properties of silicon nanocrystal LEDs. Physica E: Low-Dimensional Systems and Nanostructures, 2003, 16, 326-330.	1.3	67
143	Extending the Nanocrystal Synthesis Control to Quaternary Compositions. Crystal Growth and Design, 2012, 12, 1085-1090.	1.4	67
144	Analysis of ion beam induced damage and amorphization of 6H-SiC by raman scattering. Journal of Electronic Materials, 1996, 25, 541-547.	1.0	66

#	Article	IF	CITATIONS
145	Study of La and Cu influence on the growth inhibition and phase transformation of nano-TiO2 used for gas sensors. Sensors and Actuators B: Chemical, 2004, 100, 256-260.	4.0	66
146	Raman microprobe characterization of electrodeposited S-rich Culn(S,Se)2 for photovoltaic applications: Microstructural analysis. Journal of Applied Physics, 2007, 101, 103517.	1.1	66
147	Synthesis of SnO2 and ZnO Colloidal Nanocrystals from the Decomposition of Tin(II) 2-Ethylhexanoate and Zinc(II) 2-Ethylhexanoate. Chemistry of Materials, 2005, 17, 6468-6472.	3.2	65
148	Location and catalytic role of iron species in TiO2:Fe photocatalysts: An EPR study. Journal of Photochemistry and Photobiology A: Chemistry, 2010, 211, 170-175.	2.0	65
149	Pd ₂ Sn [010] nanorods as a highly active and stable ethanol oxidation catalyst. Journal of Materials Chemistry A, 2016, 4, 16706-16713.	5.2	65
150	Study of the influence of Nb content and sintering temperature on TiO2 sensing films. Thin Solid Films, 2003, 436, 90-94.	0.8	64
151	Boosting Photoelectrochemical Water Oxidation of Hematite in Acidic Electrolytes by Surface State Modification. Advanced Energy Materials, 2019, 9, 1901836.	10.2	64
152	Kinetic study of group IV nanoparticles ion beam synthesized in SiO2. Nuclear Instruments & Methods in Physics Research B, 2001, 178, 17-24.	0.6	63
153	A model for the response towards oxidizing gases of photoactivated sensors based on individual SnO2 nanowires. Physical Chemistry Chemical Physics, 2009, 11, 10881.	1.3	63
154	High-performance piezoresistive pressure sensors for biomedical applications using very thin structured membranes. Measurement Science and Technology, 1996, 7, 1195-1203.	1.4	62
155	TiO2 thin films from titanium butoxide: Synthesis, Pt addition, structural stability, microelectronic processing and gas-sensing properties. Sensors and Actuators B: Chemical, 2008, 130, 599-608.	4.0	61
156	Assessment of the thermal stability of anodic alumina membranes at high temperatures. Materials Chemistry and Physics, 2008, 111, 542-547.	2.0	61
157	Cu deficiency in multi-stage co-evaporated Cu(In,Ga)Se2 for solar cells applications: Microstructure and Ga in-depth alloying. Acta Materialia, 2010, 58, 3468-3476.	3.8	61
158	Gas detection with SnO2 sensors modified by zeolite films. Sensors and Actuators B: Chemical, 2007, 124, 99-110.	4.0	60
159	High-power positive electrode based on synergistic effect of N- and WO3 -decorated carbon felt for vanadium redox flow batteries. Carbon, 2018, 136, 444-453.	5.4	60
160	Microwave processing for the low cost, mass production of undoped and in situ catalytic doped nanosized SnO2 gas sensor powders. Sensors and Actuators B: Chemical, 2000, 64, 65-69.	4.0	59
161	Water vapor detection with individual tin oxide nanowires. Nanotechnology, 2007, 18, 424016.	1.3	59
162	Tuning the Fermi Level and the Kinetics of Surface States of TiO ₂ Nanorods by Means of Ammonia Treatments. Journal of Physical Chemistry C, 2013, 117, 20517-20524.	1.5	59

Joan R Morante

#	Article	IF	CITATIONS
163	Copper (II) oxide nanowires for p-type conductometric NH3 sensing. Applied Surface Science, 2014, 311, 177-181.	3.1	59
164	One-dimensional CuO–SnO2 p–n heterojunctions for enhanced detection of H2S. Journal of Materials Chemistry A, 2013, 1, 11261.	5.2	58
165	Preparation of copper oxide nanowire-based conductometric chemical sensors. Sensors and Actuators B: Chemical, 2013, 182, 7-15.	4.0	58
166	Hydrogenâ€Treated Rutile TiO ₂ Shell in Graphiteâ€Core Structure as a Negative Electrode for Highâ€Performance Vanadium Redox Flow Batteries. ChemSusChem, 2017, 10, 2089-2098.	3.6	58
167	Microstructure and secondary phases in coevaporated CuInS2 films: Dependence on growth temperature and chemical composition. Journal of Vacuum Science and Technology A: Vacuum, Surfaces and Films, 2001, 19, 232-239.	0.9	57
168	NH[sub 3] Interaction with Catalytically Modified Nano-WO[sub 3] Powders for Gas Sensing Applications. Journal of the Electrochemical Society, 2003, 150, H72.	1.3	57
169	Fabrication of metallic contacts to nanometre-sized materials using a focused ion beam (FIB). Materials Science and Engineering C, 2006, 26, 1063-1066.	3.8	57
170	Control of the doping concentration, morphology and optoelectronic properties of vertically aligned chlorine-doped ZnO nanowires. Acta Materialia, 2011, 59, 6790-6800.	3.8	57
171	Engineering the TiO2 outermost layers using magnesium for carbon dioxide photoreduction. Applied Catalysis B: Environmental, 2014, 150-151, 57-62.	10.8	57
172	Depth dependence of stress and porosity in porous silicon: a micro-Raman study. Thin Solid Films, 1999, 349, 293-297.	0.8	56
173	Residual Stress Measurement on a MEMS Structure With High-Spatial Resolution. Journal of Microelectromechanical Systems, 2007, 16, 365-372.	1.7	56
174	On the role of WO3 surface hydroxyl groups for the photocatalytic partial oxidation of methane to methanol. Catalysis Communications, 2015, 58, 200-203.	1.6	56
175	Analysis of the interfacial characteristics of BiVO ₄ /metal oxide heterostructures and its implication on their junction properties. Physical Chemistry Chemical Physics, 2019, 21, 5086-5096.	1.3	56
176	A fast preparation technique for high-quality plan view and cross-section TEM specimens of semiconducting materials. Ultramicroscopy, 1989, 31, 183-192.	0.8	55
177	Determination of micromechanical properties of thin films by beam bending measurements with an atomic force microscope. Sensors and Actuators A: Physical, 1999, 74, 134-138.	2.0	55
178	Nanocomposites SnO2/Fe2O3: Wet chemical synthesis and nanostructure characterization. Sensors and Actuators B: Chemical, 2005, 109, 64-74.	4.0	55
179	Optical and electrical properties of Si-nanocrystals ion beam synthesized in SiO2. Nuclear Instruments & Methods in Physics Research B, 2004, 216, 213-221.	0.6	54
180	Process monitoring of chalcopyrite photovoltaic technologies by Raman spectroscopy: an application to low cost electrodeposition based processes. New Journal of Chemistry, 2011, 35, 453-460.	1.4	52

#	Article	IF	CITATIONS
181	Interaction Mechanisms of Ammonia and Tin Oxide: A Combined Analysis Using Single Nanowire Devices and DFT Calculations. Journal of Physical Chemistry C, 2013, 117, 3520-3526.	1.5	52
182	Ionâ€beam synthesis of amorphous SiC films: Structural analysis and recrystallization. Journal of Applied Physics, 1996, 79, 6907-6913.	1.1	51
183	Atomic Force Microscopy Study of the Silicon Doping Influence on the First Stages of Platinum Electroless Deposition. Journal of the Electrochemical Society, 1997, 144, 909-914.	1.3	51
184	Microstructure and morphology of tin dioxide multilayer thin film gas sensors. Sensors and Actuators B: Chemical, 1997, 44, 268-274.	4.0	51
185	Electrochemical Characterization of the Open-Circuit Deposition of Platinum on Silicon from Fluoride Solutions. Journal of Physical Chemistry B, 2003, 107, 6454-6461.	1.2	51
186	Transition metals (Co, Cu) as additives on hydrothermally treated Tio2 for gas sensing. Sensors and Actuators B: Chemical, 2005, 109, 7-12.	4.0	51
187	Raman scattering and structural analysis of electrodeposited CuInSe ₂ and Sâ€rich quaternary CuIn(S,Se) ₂ semiconductors for solar cells. Physica Status Solidi (A) Applications and Materials Science, 2009, 206, 1001-1004.	0.8	51
188	Detection of amines with chromium-doped WO3 mesoporous material. Sensors and Actuators B: Chemical, 2009, 140, 557-562.	4.0	51
189	Tailored graphene materials by chemical reduction of graphene oxides of different atomic structure. RSC Advances, 2012, 2, 9643.	1.7	51
190	Charge Transfer Characterization of ALD-Grown TiO ₂ Protective Layers in Silicon Photocathodes. ACS Applied Materials & Interfaces, 2017, 9, 17932-17941.	4.0	51
191	High-power nitrided TiO2 carbon felt as the negative electrode for all-vanadium redox flow batteries. Carbon, 2019, 148, 91-104.	5.4	51
192	Robust Lithium–Sulfur Batteries Enabled by Highly Conductive WSe ₂ â€Based Superlattices with Tunable Interlayer Space. Advanced Functional Materials, 2022, 32, .	7.8	51
193	CO–CH4 selectivity enhancement by in situ Pd-catalysed microwave SnO2 nanoparticles for gas detectors using active filter. Sensors and Actuators B: Chemical, 2001, 78, 151-160.	4.0	50
194	Growth process monitoring and crystalline quality assessment of CuInS(Se)2 based solar cells by Raman spectroscopy. Thin Solid Films, 2003, 431-432, 122-125.	0.8	50
195	Vibrational energy scavenging with Si technology electromagnetic inertial microgenerators. Microsystem Technologies, 2007, 13, 1655-1661.	1.2	50
196	On the photoconduction properties of low resistivity TiO ₂ nanotubes. Nanotechnology, 2010, 21, 445703.	1.3	50
197	Optimization of surface charge transfer processes on rutile TiO2 nanorods photoanodes for water splitting. International Journal of Hydrogen Energy, 2013, 38, 2979-2985.	3.8	50
198	A practical non-enzymatic urea sensor based on NiCo ₂ O ₄ nanoneedles. RSC Advances, 2019, 9, 14443-14451.	1.7	50

#	Article	IF	CITATIONS
199	Phase Engineering of Defective Copper Selenide toward Robust Lithium–Sulfur Batteries. ACS Nano, 2022, 16, 11102-11114.	7.3	50
200	Orthorhombic Pbcn SnO2 nanowires for gas sensing applications. Journal of Crystal Growth, 2008, 310, 253-260.	0.7	49
201	Growth study of indium-catalyzed silicon nanowires by plasma enhanced chemical vapor deposition. Applied Physics A: Materials Science and Processing 2010, 100, 287-396 Carrier confinement in Gan/Ak mmi: math xmins:mmi= http://www.w3.org/1998/Math/MathML"	1.1	49

display="inline"><mml:msub><mml:mix="milline"></mml:msub></mml:msub></mml:msub></mml:math>Ga<mml:math xmlns:mml="http://www.w3.org/1998/Math/MathML" display="inline"></mml:msub></mml:msub></mml:mrow /><mml:mrow></mml:mn>1</mml:mn></mml:mo>â^^</mml:mo></mml:mi>x</mml:mi></mml:mrow></mml:msub></mml:msub></mml:math>N 202

#	Article	IF	CITATIONS
217	Raman scattering structural evaluation of CuInS2 thin films. Thin Solid Films, 2001, 387, 216-218.	0.8	45
218	Distributions of noble metal Pd and Pt in mesoporous silica. Applied Physics Letters, 2002, 81, 3449-3451.	1.5	45
219	First-Principles Study of NO[sub x] and SO[sub 2] Adsorption onto SnO[sub 2](110). Journal of the Electrochemical Society, 2007, 154, H675.	1.3	45
220	Facing Seawater Splitting Challenges by Regeneration with Ni <i>â^'</i> Mo <i>â^'</i> Fe Bifunctional Electrocatalyst for Hydrogen and Oxygen Evolution. ChemSusChem, 2021, 14, 2872-2881.	3.6	45
221	Parameter optimisation in SnO2 gas sensors for NO2 detection with low cross-sensitivity to CO: sol–gel preparation, film preparation, powder calcination, doping and grinding. Sensors and Actuators B: Chemical, 2000, 65, 166-168.	4.0	44
222	Structural, optical, and electrical properties of nanocrystalline silicon films deposited by hydrogen plasma sputtering. Journal of Vacuum Science & Technology an Official Journal of the American Vacuum Society B, Microelectronics Processing and Phenomena, 1998, 16, 1851.	1.6	43
223	Thermal modeling and management in ultrathin chip stack technology. IEEE Transactions on Components and Packaging Technologies, 2002, 25, 244-253.	1.4	43
224	Development and application of micromachined Pd/SnO2 gas sensors with zeolite coatings. Sensors and Actuators B: Chemical, 2008, 133, 435-441.	4.0	43
225	Investigation of compositional inhomogeneities in complex polycrystalline Cu(In,Ga)Se2 layers for solar cells. Applied Physics Letters, 2009, 95, .	1.5	43
226	Lowâ€ŧemperature sputtered mixtures of highâ€i⁰ and high bandgap dielectrics for GIZO TFTs. Journal of the Society for Information Display, 2010, 18, 762-772.	0.8	43
227	Growth Kinetics of Asymmetric Bi2S3 Nanocrystals: Size Distribution Focusing in Nanorods. Journal of Physical Chemistry C, 2011, 115, 7947-7955.	1.5	43
228	Miniaturized ionization gas sensors from single metal oxide nanowires. Nanoscale, 2011, 3, 630-634.	2.8	43
229	Quasi-double-star nickel and iron active sites for high-efficiency carbon dioxide electroreduction. Energy and Environmental Science, 2021, 14, 4847-4857.	15.6	43
230	Raman microstructural analysis of silicon-on-insulator formed by high dose oxygen ion implantation: As-implanted structures. Journal of Applied Physics, 1997, 82, 3730-3735.	1.1	42
231	Measurement of micromechanical properties of polysilicon microstructures with an atomic force microscope. Sensors and Actuators A: Physical, 1998, 67, 215-219.	2.0	42
232	Properties of nitrogen doped silicon films deposited by low-pressure chemical vapor deposition from silane and ammonia. Journal of Vacuum Science and Technology A: Vacuum, Surfaces and Films, 2000, 18, 2389.	0.9	42
233	SnO2/MoO3-nanostructure and alcohol detection. Sensors and Actuators B: Chemical, 2006, 118, 156-162.	4.0	42
234	Characterization of metal-oxide nanosensors fabricated with focused ion beam (FIB). Sensors and Actuators B: Chemical, 2006, 118, 198-203.	4.0	42

#	Article	IF	CITATIONS
235	Design and implementation of mechanical resonators for optimized inertial electromagnetic microgenerators. Microsystem Technologies, 2008, 14, 653-658.	1.2	42
236	Harnessing self-heating in nanowires for energy efficient, fully autonomous and ultra-fast gas sensors. Sensors and Actuators B: Chemical, 2010, 144, 1-5.	4.0	42
237	Preparation of Cr-Doped TiO2Thin Film of P-type Conduction for Gas Sensor Application. Chemistry Letters, 2002, 31, 892-893.	0.7	41
238	Measurement of residual stresses in micromachined structures in a microregion. Applied Physics Letters, 2006, 88, 071910.	1.5	41
239	Low-loss rib waveguides containing Si nanocrystals embedded in SiO2. Journal of Applied Physics, 2005, 97, 074312.	1.1	40
240	Solution Synthesis of Thin Films in the SnO2â^'In2O3System: A Case Study of the Mixing of Solâ^'Gel and Metal-Organic Solution Processes. Chemistry of Materials, 2006, 18, 840-846.	3.2	40
241	Oxygen sensing with mesoporous ceria–zirconia solid solutions. Sensors and Actuators B: Chemical, 2009, 140, 216-221.	4.0	40
242	In-depth resolved Raman scattering analysis of secondary phases in Cu-poor CuInSe2 based thin films. Applied Physics Letters, 2009, 95, 121907.	1.5	40
243	Crystallographic characterization of In2O3 films deposited by spray pyrolysis. Sensors and Actuators B: Chemical, 2002, 84, 37-42.	4.0	39
244	Chloro-Alkoxide Route to Transition Metal Oxides. Synthesis of WO ₃ Thin Films and Powders from a Tungsten Chloro-Methoxide. Chemistry of Materials, 2009, 21, 5215-5221.	3.2	39
245	A photoelectrochemical flow cell design for the efficient CO2 conversion to fuels. Electrochimica Acta, 2017, 240, 225-230.	2.6	39
246	Tailoring Copper Foam with Silver Dendrite Catalysts for Highly Selective Carbon Dioxide Conversion into Carbon Monoxide. ACS Applied Materials & Interfaces, 2018, 10, 43650-43660.	4.0	39
247	Visible photoluminescence of SiO2 implanted with carbon and silicon. Nuclear Instruments & Methods in Physics Research B, 1996, 120, 101-105.	0.6	38
248	Nanocrystals as Very Active Interfaces:  Ultrasensitive Room-Temperature Ozone Sensors with In ₂ O ₃ Nanocrystals Prepared by a Low-Temperature Solâ^'Gel Process in a Coordinating Environment. Journal of Physical Chemistry C, 2007, 111, 13967-13971.	1.5	38
249	Size-dependent recombination dynamics in ZnO nanowires. Applied Physics Letters, 2010, 96, .	1.5	38
250	Siteâ€Specific Axial Oxygen Coordinated FeN ₄ Active Sites for Highly Selective Electroreduction of Carbon Dioxide. Advanced Functional Materials, 2022, 32, .	7.8	38
251	Selfâ€assembled quantum dots of InSb grown on InP by atomic layer molecular beam epitaxy: Morphology and strain relaxation. Applied Physics Letters, 1996, 69, 3887-3889.	1.5	37
252	Electroless Addition of Catalytic Pd to SnO2Nanopowders. Chemistry of Materials, 2001, 13, 4362-4366.	3.2	37

#	Article	IF	CITATIONS
253	New method to obtain stable small-sized SnO2 powders for gas sensors. Sensors and Actuators B: Chemical, 1999, 58, 360-364.	4.0	36
254	Capping Ligand Effects on the Amorphous-to-Crystalline Transition of CdSe Nanoparticles. Langmuir, 2008, 24, 11182-11188.	1.6	36
255	Synthesis and optical spectroscopy of ZnO nanowires. Superlattices and Microstructures, 2009, 45, 271-276.	1.4	36
256	Studies on Surface Facets and Chemical Composition of Vapor Grown One-Dimensional Magnetite Nanostructures. Crystal Growth and Design, 2009, 9, 1077-1081.	1.4	36
257	Solid electrolyte interphase in semi-solid flow batteries: a wolf in sheep's clothing. Chemical Communications, 2015, 51, 14973-14976.	2.2	36
258	Synthetic natural gas production from biogas in a waste water treatment plant. Renewable Energy, 2020, 146, 1301-1308.	4.3	36
259	A new method to analyse signal transients in chemical sensors. Sensors and Actuators B: Chemical, 1994, 18, 308-312.	4.0	35
260	High temperature degradation of Pt/Ti electrodes in micro-hotplate gas sensors. Journal of Micromechanics and Microengineering, 2003, 13, S119-S124.	1.5	35
261	Gas-sensing properties of sprayed films of (CdO)/sub x/(ZnO)/sub 1-x/ mixed oxide. IEEE Sensors Journal, 2005, 5, 48-52.	2.4	35
262	Upscaling high activity oxygen evolution catalysts based on CoFe2O4 nanoparticles supported on nickel foam for power-to-gas electrochemical conversion with energy efficiencies above 80%. Applied Catalysis B: Environmental, 2019, 259, 118055.	10.8	35
263	Optical behavior of theUband in relation to EL2 and EL6 levels in boronâ€implanted GaAs. Applied Physics Letters, 1986, 48, 1138-1140.	1.5	34
264	Stress measurement by microRaman spectroscopy of polycrystalline silicon structures. Journal of Micromechanics and Microengineering, 1995, 5, 132-135.	1.5	34
265	Nondestructive assessment of the grain size distribution of SnO2 nanoparticles by low-frequency Raman spectroscopy. Applied Physics Letters, 1997, 71, 1957-1959.	1.5	34
266	Influence of the completion of oxidation on the long-term response of RGTO SnO2 gas sensors. Sensors and Actuators B: Chemical, 2000, 66, 40-42.	4.0	34
267	Thermo-mechanical analysis of micro-drop coated gas sensors. Sensors and Actuators A: Physical, 2002, 97-98, 379-385.	2.0	34
268	Chemical synthesis of In2O3 nanocrystals and their application in highly performing ozone-sensing devices. Sensors and Actuators B: Chemical, 2008, 130, 483-487.	4.0	34
269	Analysis of S-rich Culn(S,Se)2 layers for photovoltaic applications: Influence of the sulfurization temperature on the crystalline properties of electrodeposited and sulfurized CuInSe2 precursors. Journal of Applied Physics, 2008, 103, 123109.	1.1	34
270	Colloidal Counterpart of the TiO ₂ -Supported V ₂ O ₅ System: A Case Study of Oxide-on-Oxide Deposition by Wet Chemical Techniques. Synthesis, Vanadium Speciation, and Gas-Sensing Enhancement. Journal of Physical Chemistry C, 2013, 117, 20697-20705.	1.5	34

Joan R Morante

#	Article	IF	CITATIONS
271	Fe ₃ O ₄ @NiFe _{<i>x</i>} O _{<i>y</i>} Nanoparticles with Enhanced Electrocatalytic Properties for Oxygen Evolution in Carbonate Electrolyte. ACS Applied Materials & Interfaces, 2016, 8, 29461-29469.	4.0	34
272	NH3 sensing with self-assembled ZnO-nanowire μHP sensors in isothermal and temperature-pulsed mode. Sensors and Actuators B: Chemical, 2016, 226, 110-117.	4.0	34
273	Spectroscopic characterization of phases formed by highâ€dose carbon ion implantation in silicon. Journal of Applied Physics, 1995, 77, 2978-2984.	1.1	33
274	Analysis of geometrical effects on the behavior of transverse and longitudinal modes of amorphous silicon compounds. Journal of Applied Physics, 1997, 81, 1933-1942.	1.1	33
275	Direct observation of the gas-surface interaction kinetics in nanowires through pulsed self-heating assisted conductometric measurements. Applied Physics Letters, 2009, 95, .	1.5	33
276	Visible Photoluminescence Components of Solution-Grown ZnO Nanowires: Influence of the Surface Depletion Layer. Journal of Physical Chemistry C, 2012, 116, 19496-19502.	1.5	33
277	Surface modification of metal oxide nanocrystals for improved supercapacitors. Energy and Environmental Science, 2012, 5, 7555.	15.6	33
278	Static and Dynamic Studies on LiNi _{1/3} Co _{1/3} Mn _{1/3} O ₂ â€Based Suspensions for Semiâ€Solid Flow Batteries. ChemSusChem, 2016, 9, 1938-1944.	3.6	33
279	Combined in-depth scanning Auger microscopy and Raman scattering characterisation of CulnS2 polycrystalline films. Vacuum, 2001, 63, 315-321.	1.6	32
280	Conductivity Dependence on Oxygen Partial Pressure and Oxide-Ion Transport Numbers Determination for La[sub 2]Mo[sub 2]O[sub 9]. Electrochemical and Solid-State Letters, 2004, 7, A373.	2.2	32
281	Size dependence of refractive index of Si nanoclusters embedded in SiO2. Journal of Applied Physics, 2005, 98, 013523.	1.1	32
282	The role of source and drain material in the performance of GIZO based thinâ€film transistors. Physica Status Solidi (A) Applications and Materials Science, 2008, 205, 1905-1909.	0.8	32
283	Acetone sensors based on TiO2 nanocrystals modified with tungsten oxide species. Journal of Alloys and Compounds, 2016, 665, 345-351.	2.8	32
284	Different Behavior in the Deposition of Platinum from HF Solutions on n―and pâ€Type (100) Si Substrates. Journal of the Electrochemical Society, 1997, 144, 4119-4122.	1.3	31
285	Deposition on micromachined silicon substrates of gas sensitive layers obtained by a wet chemical route: a CO/CH4 high performance sensor. Thin Solid Films, 2001, 391, 265-269.	0.8	31
286	Gas-sensing properties of catalytically modified WO/sub 3/ with copper and vanadium for NH/sub 3/ detection. IEEE Sensors Journal, 2005, 5, 385-391.	2.4	31
287	Raman scattering characterisation of electrochemical growth of CuInSe ₂ nanocrystalline thin films for photovoltaic applications: Surface and inâ€depth analysis. Surface and Interface Analysis, 2008, 40, 798-801.	0.8	31
288	An array of ordered pillars with retentive properties for pressure-driven liquid chromatography fabricated directly from an unmodified cyclo olefin polymer. Lab on A Chip, 2009, 9, 1511.	3.1	31

#	Article	IF	CITATIONS
289	Turning Earth Abundant Kesterite-Based Solar Cells Into Efficient Protected Water-Splitting Photocathodes. ACS Applied Materials & Interfaces, 2018, 10, 13425-13433.	4.0	31
290	Concerning the 506cmâ^'1 band in the Raman spectrum of silicon nanowires. Applied Physics Letters, 2007, 91, 123107.	1.5	30
291	On the structural characterization of BaTiO3–CuO as CO2 sensing material. Sensors and Actuators B: Chemical, 2008, 133, 315-320.	4.0	30
292	Quantitative analysis of CO-humidity gas mixtures with self-heated nanowires operated in pulsed mode. Applied Physics Letters, 2010, 97, .	1.5	30
293	Bottom-up processing of thermoelectric nanocomposites from colloidal nanocrystal building blocks: the case of Ag2Te–PbTe. Journal of Nanoparticle Research, 2012, 14, 1.	0.8	30
294	Effects of solar irradiation on thermally driven CO2 methanation using Ni/CeO2–based catalyst. Applied Catalysis B: Environmental, 2021, 291, 120038.	10.8	30
295	Thermal emission rates and capture cross-section of majority carriers at titanium levels in silicon. Solid-State Electronics, 1983, 26, 1-6.	0.8	29
296	Thick polycrystalline silicon for surface-micromechanical applications: deposition, structuring and mechanical characterization. Sensors and Actuators A: Physical, 1996, 54, 674-678.	2.0	29
297	Properties of nanocrystalline SnO2 obtained by means of a microwave process. Materials Science and Engineering C, 2001, 15, 203-205.	3.8	29
298	Control of tunnel oxide thickness in Si-nanocrystal array memories obtained by ion implantation and its impact in writing speed and volatility. Applied Physics Letters, 2003, 82, 2151-2153.	1.5	29
299	Time-resolved analysis of the white photoluminescence from SiO2 films after Si and C coimplantation. Applied Physics Letters, 2004, 84, 25-27.	1.5	29
300	Mechanical and NH3 sensing properties of long multi-walled carbon nanotube ropes. Carbon, 2006, 44, 1821-1825.	5.4	29
301	Key role of Cu–Se binary phases in electrodeposited CuInSe2 precursors on final distribution of Cu–S phases in CuIn(S,Se)2 absorbers. Thin Solid Films, 2009, 517, 2268-2271.	0.8	29
302	Bidimensional versus tridimensional oxygen vacancy diffusion in SnO2â^'x under different gas environments. Physical Chemistry Chemical Physics, 2010, 12, 2401.	1.3	29
303	Raman scattering analysis of Cu-poor Cu(In,Ga)Se2 cells fabricated on polyimide substrates: Effect of Na content on microstructure and phase structure. Thin Solid Films, 2011, 519, 7300-7303.	0.8	29
304	Anisotropic magnetoresistance of individual CoFeB and Ni nanotubes with values of up to 1.4% at room temperature. APL Materials, 2014, 2, .	2.2	29
305	Insight into the Degradation Mechanisms of Atomic Layer Deposited TiO2 as Photoanode Protective Layer. ACS Applied Materials & Interfaces, 2019, 11, 29725-29735.	4.0	29
306	Effects of prior hydrogenation on the structure and properties of thermally nanocrystallized silicon layers. Journal of Applied Physics, 1998, 83, 5797-5803.	1.1	28

Joan R Morante

#	Article	IF	CITATIONS
307	Electroless Addition of Platinum to SnO2Nanopowders. Chemistry of Materials, 2002, 14, 3277-3283.	3.2	28
308	The effect of additional oxidation on the memory characteristics of metal-oxide-semiconductor capacitors with Si nanocrystals. Applied Physics Letters, 2003, 82, 4818-4820.	1.5	28
309	Analyses of the ammonia response of integrated gas sensors working in pulsed mode. Sensors and Actuators B: Chemical, 2006, 118, 318-322.	4.0	28
310	Ab initio insights into the visible luminescent properties of ZnO. Thin Solid Films, 2007, 515, 8670-8673.	0.8	28
311	Operando studies of all-vanadium flow batteries: Easy-to-make reference electrode based on silver–silver sulfate. Journal of Power Sources, 2014, 271, 556-560.	4.0	28
312	Unusual photoluminescence properties in amorphous silicon nanopowder produced by plasma enhanced chemical vapor deposition. Applied Physics Letters, 1994, 64, 463-465.	1.5	27
313	Low temperature direct growth of nanocrystalline silicon carbide films. Materials Science and Engineering B: Solid-State Materials for Advanced Technology, 2000, 69-70, 530-535.	1.7	27
314	Comparative structural study between sputtered and liquid pyrolysis nanocrystaline SnO2. Materials Science and Engineering B: Solid-State Materials for Advanced Technology, 2000, 69-70, 406-410.	1.7	27
315	Performances of La–TiO2 nanoparticles as gas sensing material. Sensors and Actuators B: Chemical, 2005, 111-112, 7-12.	4.0	27
316	Direct imaging of the visible emission bands from individual ZnO nanowires by near-field optical spectroscopy. Nanotechnology, 2009, 20, 315701.	1.3	27
317	Assessment of absorber composition and nanocrystalline phases in CuInS2 based photovoltaic technologies by ex-situ/in-situ resonant Raman scattering measurements. Solar Energy Materials and Solar Cells, 2011, 95, S83-S88.	3.0	27
318	Solution-growth and optoelectronic performance of ZnO : Cl/TiO ₂ and ZnO : Cl/Zn _x TiO _y /TiO ₂ core–shell nanowires with tunable shell thickness. Journal Physics D: Applied Physics, 2012, 45, 415301.	1.3	27
319	Facile integration of ordered nanowires in functional devices. Sensors and Actuators B: Chemical, 2015, 221, 104-112.	4.0	27
320	Molecular Engineering to Tune the Ligand Environment of Atomically Dispersed Nickel for Efficient Alcohol Electrochemical Oxidation. Advanced Functional Materials, 2021, 31, 2106349.	7.8	27
321	Structural damage and defects created in SiO2 films by Ar ion implantation. Journal of Non-Crystalline Solids, 1995, 187, 101-105.	1.5	26
322	Magnetron sputtering synthesis of silicon–carbon films: structural and optical characterization. Solid-State Electronics, 1998, 42, 2315-2320.	0.8	26
323	Built-in active filter for an improved response to carbon monoxide combining thin- and thick-film technologies. Sensors and Actuators B: Chemical, 2002, 87, 88-94.	4.0	26
324	Oxide nanopowders from the low-temperature processing of metal oxide sols and their application as gas-sensing materials. Sensors and Actuators B: Chemical, 2006, 118, 105-109.	4.0	26

#	Article	IF	CITATIONS
325	Pt doping triggers growth of TiO2 nanorods: nanocomposite synthesis and gas-sensing properties. CrystEngComm, 2012, 14, 3882.	1.3	26
326	Reconstruction of the SiO2structure damaged by low-energy Ar-implanted ions. Journal of Applied Physics, 1997, 81, 126-134.	1.1	25
327	Single crystalline and core–shell indium-catalyzed germanium nanowires—a systematic thermal CVD growth study. Nanotechnology, 2009, 20, 245608.	1.3	25
328	Synthesis of Ceria–Zirconia Nanocrystals with Improved Microstructural Homogeneity and Oxygen Storage Capacity by Hydrolytic Sol–Gel Process in Coordinating Environment. Advanced Functional Materials, 2012, 22, 2867-2875.	7.8	25
329	Solution-growth and optoelectronic properties of ZnO:Cl@ZnS core–shell nanowires with tunable shell thickness. Journal of Alloys and Compounds, 2013, 555, 213-218.	2.8	25
330	Ion-beam synthesis and structural characterization of ZnS nanocrystals in SiO2. Applied Physics Letters, 1998, 72, 3488-3490.	1.5	24
331	Enhancement of the emission yield of silicon nanocrystals in silica due to surface passivation. Physica E: Low-Dimensional Systems and Nanostructures, 2003, 16, 424-428.	1.3	24
332	Surface states in template synthesized tin oxide nanoparticles. Journal of Applied Physics, 2004, 95, 2178-2180.	1.1	24
333	Enhancement of the photoelectrochemical properties of Cl-doped ZnO nanowires by tuning their coaxial doping profile. Applied Physics Letters, 2011, 99, .	1.5	24
334	Catalyst size limitation in vapor–liquid–solid ZnO nanowire growth using pulsed laser deposition. Thin Solid Films, 2012, 520, 4626-4631.	0.8	24
335	Enhanced Photovoltaic Performance of Nanowire Dye-Sensitized Solar Cells Based on Coaxial TiO ₂ @TiO Heterostructures with a Cobalt(II/III) Redox Electrolyte. ACS Applied Materials & Interfaces, 2013, 5, 9872-9877.	4.0	24
336	Photocatalytic Hydrogen Evolution Using Bi-Metallic (Ni/Pt) Na2Ti3O7 Whiskers: Effect of the Deposition Order. Catalysts, 2019, 9, 285.	1.6	24
337	Quantum wirelike induced morphology in InGaAs wells grown on InyAl1â~'yAs tensile buffer layers over (100)InP vicinal surfaces. Applied Physics Letters, 1995, 66, 2391-2393.	1.5	23
338	The Role of Chemical Species in the Passivation of 〈100〉 Silicon Surfaces by HF in Waterâ€Ethanol Solutions. Journal of the Electrochemical Society, 1996, 143, 4059-4066.	1.3	23
339	Substrate temperature dependence of the photoluminescence efficiency of co-sputtered Si/SiO2 layers. Journal of Luminescence, 1998, 80, 241-245.	1.5	23
340	Properties of SiOxNy films deposited by LPCVD from SiH4/N2O/NH3 gaseous mixture. Sensors and Actuators A: Physical, 1999, 74, 52-55.	2.0	23
341	Modification of surface mechanical properties of polycarbonate by ion implantation. Surface and Coatings Technology, 2002, 158-159, 636-642.	2.2	23
342	Copper oxide nanowires prepared by thermal oxidation for chemical sensing. Procedia Engineering, 2011, 25, 753-756.	1.2	23

#	Article	IF	CITATIONS
343	Insights into the Performance of Co _{<i>x</i>} Ni _{1–<i>x</i>} TiO ₃ Solid Solutions as Photocatalysts for Sun-Driven Water Oxidation. ACS Applied Materials & Interfaces, 2017, 9, 40290-40297.	4.0	23
344	Solar vanadium redox-flow battery powered by thin-film silicon photovoltaics for efficient photoelectrochemical energy storage. Journal Physics D: Applied Physics, 2019, 52, 044001.	1.3	23
345	Influence of the composition modulation on the relaxation of In0.54Ga0.46As strained layers. Applied Physics Letters, 1991, 59, 1957-1959.	1.5	22
346	Analysis of the Thermal Oxidation of Tin Droplets and Its Implications on Gas Sensor Stability. Journal of the Electrochemical Society, 1999, 146, 3527-3535.	1.3	22
347	Structural and gas-sensing properties of WO/sub 3/ nanocrystalline powders obtained by a sol-gel method from tungstic acid. IEEE Sensors Journal, 2002, 2, 329-335.	2.4	22
348	DRIFTS analysis of the CO2 detection mechanisms using LaOCl sensing material. Sensors and Actuators B: Chemical, 2005, 108, 484-489.	4.0	22
349	Effectiveness of nitrogen incorporation to enhance the photoelectrochemical activity of nanostructured TiO ₂ :NH ₃ versus H ₂ –N ₂ annealing. Nanotechnology, 2011, 22, 235403.	1.3	22
350	Structure of 60Ű dislocations at the GaAs/Si interface. Journal of Applied Physics, 1996, 79, 676.	1.1	21
351	Dynamic simulations of micropumps. Journal of Micromechanics and Microengineering, 1996, 6, 128-130.	1.5	21
352	Synthesis of SiC Microstructures in Si Technology by High Dose Carbon Implantation: Etchâ€Stop Properties. Journal of the Electrochemical Society, 1997, 144, 2211-2215.	1.3	21
353	Black-body emission from nanostructured materials. Journal of Luminescence, 1998, 80, 519-522.	1.5	21
354	Synthesis of Tin Oxide Nanostructures with Controlled Particle Size Using Mesoporous Frameworks. Electrochemical and Solid-State Letters, 2004, 7, G93.	2.2	21
355	Electrodeposition based synthesis of S-rich CuIn(S,Se)2 layers for photovoltaic applications: Raman scattering analysis of electrodeposited CuInSe2 precursors. Thin Solid Films, 2009, 517, 2163-2166.	0.8	21
356	Embedding catalytic nanoparticles inside mesoporous structures with controlled porosity: Au@TiO2. Journal of Materials Chemistry A, 2013, 1, 14170.	5.2	21
357	Surface Modification of TiO ₂ Nanocrystals by WO _{<i>x</i>} Coating or Wrapping: Solvothermal Synthesis and Enhanced Surface Chemistry. ACS Applied Materials & Interfaces, 2015, 7, 6898-6908.	4.0	21
358	Evidence of catalytic activation of anatase nanocrystals by vanadium oxide surface layer: Acetone and ethanol sensing properties. Sensors and Actuators B: Chemical, 2015, 217, 193-197.	4.0	21
359	A low temperature solid state reaction to produce hollow MnxFe3-xO4 nanoparticles as anode for lithium-ion batteries. Nano Energy, 2019, 66, 104199.	8.2	21
360	Optical characterization of porous silicon embedded with CdSe nanoparticles. Applied Physics Letters, 1998, 73, 2766-2768.	1.5	20

#	Article	IF	CITATIONS
361	Strain-Induced Quenching of Optical Transitions in Capped Self-Assembled Quantum Dot Structures. Physical Review Letters, 1998, 80, 1094-1097.	2.9	20
362	Optical and electrical transport mechanisms in Si-nanocrystal-based LEDs. Physica E: Low-Dimensional Systems and Nanostructures, 2003, 17, 604-606.	1.3	20
363	In situ and ex situ characterisation of thermally induced crystallisation of CuInS2 thin films for solar cell. Thin Solid Films, 2005, 480-481, 362-366.	0.8	20
364	Electrochemical synthesis of CuIn(S,Se)2 alloys with graded composition for high efficiency solar cells. Applied Physics Letters, 2009, 94, 061915.	1.5	20
365	Ultraviolet Raman scattering in ZnO nanowires: quasimode mixing and temperature effects. Journal of Raman Spectroscopy, 2011, 42, 153-159.	1.2	20
366	Three-dimensional rice husk-originated mesoporous silicon and its electrical properties. Materials Today Communications, 2018, 14, 141-150.	0.9	20
367	A novel time-domain method to analyse multicomponent exponential transients. Measurement Science and Technology, 1995, 6, 135-142.	1.4	19
368	Physical techniques for silicon layer analysis. Microelectronic Engineering, 1998, 40, 223-237.	1.1	19
369	Optical and structural characterization of Si nanocrystals ion beam synthesized in SiO2: correlation between the surface passivation and the photoluminescence emission. Solid-State Electronics, 2001, 45, 1495-1504.	0.8	19
370	Nanosized Nb-TiO/sub 2/ gas sensors derived from alkoxides hydrolization. IEEE Sensors Journal, 2003, 3, 189-194.	2.4	19
371	Electrochemical deposition of Cu and Ni/Cu multilayers in Si Microsystem Technologies. Sensors and Actuators A: Physical, 2005, 123-124, 633-639.	2.0	19
372	SnO2 thin films from metalorganic precursors: Synthesis, characterization, microelectronic processing and gas-sensing properties. Sensors and Actuators B: Chemical, 2007, 124, 217-226.	4.0	19
373	Mesoporous Silica: A Suitable Adsorbent for Amines. Nanoscale Research Letters, 2009, 4, 1303-8.	3.1	19
374	Thermally Stable Positive Electrolytes with a Superior Performance in Allâ€Vanadium Redox Flow Batteries. ChemPlusChem, 2015, 80, 354-358.	1.3	19
375	Electron Bottleneck in the Charge/Discharge Mechanism of Lithium Titanates for Batteries. ChemSusChem, 2015, 8, 1737-1744.	3.6	19
376	Light management in photoelectrochemical water splitting – from materials to device engineering. Journal of Materials Chemistry C, 2021, 9, 3726-3748.	2.7	19
377	Field influence on deep level transients at large deep to shallow trap ratios. Applied Physics Letters, 1984, 45, 1317-1319.	1.5	18
378	Passivation analysis of micromechanical silicon structures obtained by electrochemical etch stop. Sensors and Actuators A: Physical, 1993, 37-38, 744-750.	2.0	18

#	Article	IF	CITATIONS
379	Configurational statistical model for the damaged structure of silicon oxide after ion implantation. Physical Review B, 1994, 49, 14845-14849.	1.1	18
380	Stress-profile characterization and test-structure analysis of single and double ion-implanted LPCVD polycrystalline silicon. Sensors and Actuators A: Physical, 1996, 54, 718-723.	2.0	18
381	Model for efficient visible emission from Si nanocrystals ion beam synthesized in SiO2. Nuclear Instruments & Methods in Physics Research B, 2001, 178, 89-92.	0.6	18
382	Microdeposition of microwave obtained nanoscaled SnO2 powders for gas sensing microsystems. Sensors and Actuators B: Chemical, 2002, 84, 60-65.	4.0	18
383	Gadolinium doped Ceria nanocrystals synthesized from mesoporous silica. Journal of Nanoparticle Research, 2008, 10, 369-375.	0.8	18
384	Sputtered multicomponent amorphous dielectrics for transparent electronics. Physica Status Solidi (A) Applications and Materials Science, 2009, 206, 2149-2154.	0.8	18
385	Characterization of individual barium titanate nanorods and their assessment as building blocks of new circuit architectures. Nanotechnology, 2011, 22, 385501.	1.3	18
386	Assessment and Modeling of NH3-SnO2 Interactions using Individual Nanowires. Procedia Engineering, 2012, 47, 293-297.	1.2	18
387	Hydrogenation and Structuration of TiO ₂ Nanorod Photoanodes: Doping Level and the Effect of Illumination in Trap-States Filling. Journal of Physical Chemistry C, 2018, 122, 3295-3304.	1.5	18
388	Engineering Au/MnO ₂ hierarchical nanoarchitectures for ethanol electrochemical valorization. Journal of Materials Chemistry A, 2020, 8, 16902-16907.	5.2	18
389	Dependence of the electron cross section for the acceptor gold level in silicon on the gold to donor ratio. Applied Physics Letters, 1982, 41, 656-658.	1.5	17
390	Detailed analysis of Î ² -SiC formation by high dose carbon ion implantation in silicon. Materials Science and Engineering B: Solid-State Materials for Advanced Technology, 1996, 36, 282-285.	1.7	17
391	Defects, surface roughening, and anisotropy on the tensile In[sub x]Ga[sub 1â~'x]As/InP(001) system. Journal of Vacuum Science & Technology an Official Journal of the American Vacuum Society B, Microelectronics Processing and Phenomena, 1997, 15, 687.	1.6	17
392	Pulverisation method for active layer coating on microsystems. Sensors and Actuators B: Chemical, 2002, 84, 78-82.	4.0	17
393	An electrochemical study of tin oxide thin film in borate buffer solutions. Journal of the Brazilian Chemical Society, 2003, 14, 523-529.	0.6	17
394	Recombination dynamics in ZnO nanowires: Surfaces states versus mode quality factor. Applied Physics Letters, 2010, 97, .	1.5	17
395	Multilayered Hematite Nanowires with Thinâ€Film Silicon Photovoltaics in an Allâ€Earthâ€Abundant Hybrid Tandem Device for Solar Water Splitting. ChemSusChem, 2019, 12, 1428-1436.	3.6	17
396	Influence of the desorption and growth temperatures on the crystalline quality of molecular-beam epitaxy InAlAs layers. Journal of Vacuum Science & Technology an Official Journal of the American Vacuum Society B, Microelectronics Processing and Phenomena, 1992, 10, 2148.	1.6	16

#	Article	IF	CITATIONS
397	Non-destructive characterization of the uniformity of thin cobalt disilicide films by Raman microprobe measurements. Thin Solid Films, 1994, 251, 45-50.	0.8	16
398	β-SiC on SiO2 formed by ion implantation and bonding for micromechanics applications. Sensors and Actuators A: Physical, 1999, 74, 169-173.	2.0	16
399	Ostwald ripening of Ge precipitates elaborated by ion implantation in SiO2. Materials Science and Engineering B: Solid-State Materials for Advanced Technology, 2000, 69-70, 380-385.	1.7	16
400	In situ analysis of the conductance of SnO2 crystalline nanoparticles in the presence of oxidizing or reducing atmosphere by scanning tunneling microscopy. Sensors and Actuators B: Chemical, 2001, 78, 57-63.	4.0	16
401	Growth of GaN layers on SiC/Si(111) substrate by molecular beam epitaxy. Materials Science and Engineering B: Solid-State Materials for Advanced Technology, 2002, 93, 172-176.	1.7	16
402	Optical-geometrical effects on the photoluminescence spectra of Si nanocrystals embedded in SiO2. Journal of Applied Physics, 2005, 98, 084319.	1.1	16
403	Distinguishing feature of metal oxide films' structural engineering for gas sensor applications. Journal of Physics: Conference Series, 2005, 15, 256-261.	0.3	16
404	Effect of the nanostructure and surface chemistry on the gas adsorption properties of macroscopic multiwalled carbon nanotube ropes. Carbon, 2007, 45, 83-88.	5.4	16
405	Linear and non-linear behavior of mechanical resonators for optimized inertial electromagnetic microgenerators. Microsystem Technologies, 2009, 15, 1217-1223.	1.2	16
406	Metal Oxide Nanocrystals from the Injection of Metal Oxide Sols in a Coordinating Environment: Principles, Applicability, and Investigation of the Synthesis Variables in the Case Study of CeO ₂ and SnO ₂ . Chemistry of Materials, 2009, 21, 862-870.	3.2	16
407	A novel ï€-d conjugated cobalt tetraaza[14]annulene based atomically dispersed electrocatalyst for efficient CO2 reduction. Chemical Engineering Journal, 2022, 442, 136129.	6.6	16
408	Photoluminescence in silicon powder grown by plasma-enhanced chemical-vapor deposition: Evidence of a multistep-multiphoton excitation process. Physical Review B, 1994, 50, 18124-18133.	1.1	15
409	Determination of the direct band-gap energy of InAlAs matched to InP by photoluminescence excitation spectroscopy. Journal of Applied Physics, 1997, 81, 6916-6920.	1.1	15
410	Texture and stress profile in thick polysilicon films suitable for fabrication of microstructures. Thin Solid Films, 1997, 296, 177-180.	0.8	15
411	Ion beam synthesis of semiconductor nanoparticles for Si based optoelectronic devices. Nuclear Instruments & Methods in Physics Research B, 2000, 161-163, 904-908.	0.6	15
412	Mechanism of NH3 interaction with transition metal-added nanosized WO3 for gas sensing: In situ electron paramagnetic resonance study. Catalysis Today, 2007, 126, 169-176.	2.2	15
413	Synthesis and structural properties of ultra-small oxide (TiO2, ZrO2, SnO2) nanoparticles prepared by decomposition of metal alkoxides. Materials Chemistry and Physics, 2010, 124, 809-815.	2.0	15
414	Influence of NaF incorporation during Cu(In,Ga)Se <inf>2</inf> growth on microstructure and photovoltaic performance. , 2010, , .		15

#	Article	IF	CITATIONS
415	Multilayer Ni/Fe thin films as oxygen evolution catalysts for solar fuel production. Journal Physics D: Applied Physics, 2017, 50, 104003.	1.3	15
416	Modelling the rheology and electrochemical performance of Li4Ti5O12 and LiNi1/3Co1/3Mn1/3O2 based suspensions for semi-solid flow batteries. Electrochimica Acta, 2019, 304, 146-157.	2.6	15
417	Raman scattering and photoluminescence analysis of silicon on insulator structures obtained by single and multiple oxygen implants. Journal of Applied Physics, 1991, 70, 1678-1683.	1.1	14
418	Competitive evolution of the fine contrast modulation and CuPt ordering in InGaP/GaAs layers. Journal of Applied Physics, 1996, 80, 3798-3803.	1.1	14
419	Behavior of strained Si1â^'yCy (0⩽y⩽0.02) layers grown on silicon during wet oxidation. Journal of Appliec Physics, 1999, 85, 833-840.	1.1	14
420	Influence of anneals in oxygen ambient on stress of thick polysilicon layers. Sensors and Actuators A: Physical, 1999, 76, 335-342.	2.0	14
421	Structural and optical characterization of Mn doped ZnS nanocrystals elaborated by ion implantation in SiO2. Nuclear Instruments & Methods in Physics Research B, 1999, 147, 373-377.	0.6	14
422	Nanostructured oxides on porous silicon microhotplates for NH3 sensing. Microelectronic Engineering, 2008, 85, 1116-1119.	1.1	14
423	On-chip fabrication of surface ionisation gas sensors. Sensors and Actuators B: Chemical, 2013, 182, 25-30.	4.0	14
424	Influence of In and Ga additives onto SnO2 inkjet-printed semiconductor. Thin Solid Films, 2014, 553, 118-122.	0.8	14
425	Conformal chalcopyrite based photocathode for solar refinery applications. Solar Energy Materials and Solar Cells, 2016, 158, 184-188.	3.0	14
426	Adaptation of Cu(In, Ga)Se ₂ photovoltaics for full unbiased photocharge of integrated solar vanadium redox flow batteries. Sustainable Energy and Fuels, 2020, 4, 1135-1142.	2.5	14
427	Test microstructures for measurement of SiC thin film mechanical properties. Journal of Micromechanics and Microengineering, 1999, 9, 190-193.	1.5	13
428	Synthesis of luminescent particles in SiO2 films by sequential Si and C ion implantation. Microelectronics Reliability, 2000, 40, 885-888.	0.9	13
429	Absorption cross-sections and lifetimes as a function of size in Si nanocrystals embedded in SiO2. Physica E: Low-Dimensional Systems and Nanostructures, 2003, 16, 429-433.	1.3	13
430	High-density YSZ tapes fabricated via the multi-folding lamination process. Ceramics International, 2009, 35, 1219-1226.	2.3	13
431	From doping to phase transformation: Ammonia sensing performances of chloroalkoxide-derived WO3 powders modified with chromium. Sensors and Actuators B: Chemical, 2010, 148, 200-206.	4.0	13
432	Spatially resolved Raman spectroscopy on indium-catalyzed core–shell germanium nanowires: size effects. Nanotechnology, 2010, 21, 105703.	1.3	13

#	Article	IF	CITATIONS
433	Role of Bismuth in the Electrokinetics of Silicon Photocathodes for Solar Rechargeable Vanadium Redox Flow Batteries. ChemSusChem, 2018, 11, 125-129.	3.6	13
434	Gas sensing properties of individual SnO ₂ nanowires and SnO ₂ sol–gel nanocomposites. Beilstein Journal of Nanotechnology, 2019, 10, 1380-1390.	1.5	13
435	Majorityâ€carrier capture crossâ€section determination in the large deepâ€trap concentration cases. Journal of Applied Physics, 1986, 59, 1562-1569.	1.1	12
436	Influence of the silicon wafer cleaning treatment on the Si/SiO2 interfaces analyzed by infrared spectroscopy. Applied Surface Science, 1992, 56-58, 861-865.	3.1	12
437	Analysis of nonlinearity in high sensitivity piezoresistive pressure sensors. Sensors and Actuators A: Physical, 1993, 37-38, 790-795.	2.0	12
438	Electrochemical etching of porous silicon sacrificial layers for micromachining applications. Journal of Micromechanics and Microengineering, 1997, 7, 131-132.	1.5	12
439	Improvement of the porous silicon sacrificial-layer etching for micromachining applications. Sensors and Actuators A: Physical, 1997, 62, 676-679.	2.0	12
440	Innovative method of pulverisation coating of prestabilized nanopowders for mass production of gas sensors. Sensors and Actuators B: Chemical, 2001, 78, 78-82.	4.0	12
441	Thermal fatigue modeling of micromachined gas sensors. Sensors and Actuators B: Chemical, 2003, 95, 275-281.	4.0	12
442	Raman scattering microcrystalline assessment and device quality control of electrodeposited CuIn(S,Se)2 based solar cells. Thin Solid Films, 2008, 516, 7021-7025.	0.8	12
443	Synthesis of Soluble and Size-Controlled SnO2 and CeO2 Nanocrystals: Application of a General Concept for the Low-Temperature, Hydrolytic Synthesis of Organically Capped Oxide Nanoparticles. European Journal of Inorganic Chemistry, 2008, 2008, 859-862.	1.0	12
444	Analysis of sulphurisation processes of electrodeposited S-rich CuIn(S,Se)2 layers for photovoltaic applications. Thin Solid Films, 2009, 517, 2264-2267.	0.8	12
445	The Chloroalkoxide Route to Transition Metal Oxides. Synthesis of V ₂ O ₅ Thin Films and Powders from a Vanadium Chloromethoxide. Chemistry of Materials, 2009, 21, 1618-1626.	3.2	12
446	An experimental method to estimate the temperature of individual nanowires. International Journal of Nanotechnology, 2009, 6, 860.	0.1	12
447	Degradation and regeneration mechanisms of NiO protective layers deposited by ALD on photoanodes. Journal of Materials Chemistry A, 2019, 7, 21892-21902.	5.2	12
448	Quasi-1D Mn ₂ O ₃ Nanostructures Functionalized with First-Row Transition-Metal Oxides as Oxygen Evolution Catalysts. ACS Applied Nano Materials, 2020, 3, 9889-9898.	2.4	12
449	Analysis of Thermal Capture of the Acceptor Level of Gold in Silicon. Physica Status Solidi (B): Basic Research, 1982, 111, 375-382.	0.7	11
450	Analysis by FT-IR spectroscopy of SiO2-polycrystalline structures used in micromechanics: Stress measurements. Sensors and Actuators A: Physical, 1992, 32, 347-353.	2.0	11

#	Article	IF	CITATIONS
451	Etching rate modification in silicon oxide by ion implantation and rapid thermal annealing. Nuclear Instruments & Methods in Physics Research B, 1993, 80-81, 1367-1370.	0.6	11
452	Fine speckle contrast in InGaAs/InP systems: Influence of layer thickness, mismatch, and growth temperature. Journal of Applied Physics, 1993, 73, 4319-4323.	1.1	11
453	Surface step bunching and crystal defects in InAlAs films grown by molecular beam epitaxy on (111)B InP substrates. Applied Physics Letters, 1997, 71, 2961-2963.	1.5	11
454	Sulfurization of Cu/In Precursors for CuInS[sub 2]-Based Solar Cells. Journal of the Electrochemical Society, 2003, 150, G400.	1.3	11
455	Chemical to electrical transduction mechanisms from single metal oxide nanowire measurements: response time constant analysis. Nanotechnology, 2013, 24, 444004.	1.3	11
456	Acetone Sensing with TiO2-WO3 Nanocomposites: An Example of Response Enhancement by Inter-oxide Cooperative Effects. Procedia Engineering, 2014, 87, 803-806.	1.2	11
457	On the role of Cu, Ag and Pt in active titania for gas-phase ethanol photo-reforming. Materials Science in Semiconductor Processing, 2018, 73, 30-34.	1.9	11
458	Analysis of a reverse-biased linearly graded junction with high concentration of deep impurities. Solid-State Electronics, 1990, 33, 805-811.	0.8	10
459	On the artificial creation of the EL2 center by means of boron implantation in gallium arsenide. Journal of Applied Physics, 1991, 70, 4202-4210.	1.1	10
460	Raman characterization of SOI-SIMOX structures. Materials Letters, 1992, 15, 122-126.	1.3	10
461	Analysis of electrostatic-damped piezoresistive silicon accelerometers. Sensors and Actuators A: Physical, 1993, 37-38, 317-322.	2.0	10
462	Atomic scale study of the interaction between misfit dislocations at the GaAs/Si interface. Applied Physics Letters, 1996, 68, 1244-1246.	1.5	10
463	Thermal dry oxidation of Si1-x-yGexCy strained layers grown on silicon. Microelectronic Engineering, 1999, 48, 207-210.	1.1	10
464	Oxidation of Si1â^'xâ^'yGexCy strained layers grown on Si: kinetics and interface properties. Microelectronics Reliability, 2000, 40, 829-832.	0.9	10
465	Effect of implantation and annealing conditions on the photoluminescence emission of Si nanocrystals ion beam synthesised in SiO2. Microelectronics Reliability, 2000, 40, 859-862.	0.9	10
466	Characterisation and stabilisation of Pt/TaSix/SiO2/SiC gas sensor. Sensors and Actuators B: Chemical, 2005, 109, 119-127.	4.0	10
467	Mechanical characterization of thermal flow sensors membranes. Sensors and Actuators A: Physical, 2006, 125, 260-266.	2.0	10
468	Si technology based microinductive devices for biodetection applications. Sensors and Actuators A: Physical, 2006, 132, 499-505.	2.0	10

#	Article	IF	CITATIONS
469	Sensing sensibility of surface micromachined suspended gate polysilicon thin film transistors. Sensors and Actuators B: Chemical, 2006, 118, 243-248.	4.0	10
470	Effect of grain size distribution on the grain boundary electrical response of 2D and 3D polycrystals. Solid State Ionics, 2006, 177, 3117-3121.	1.3	10
471	Growth of CdSe Nanocrystals by a Catalytic Redox Activation of Ostwald Ripening:  A Case Study of the Concept of Traveling Solubility Perturbation. Chemistry of Materials, 2007, 19, 4919-4924.	3.2	10
472	Chemoresistive sensing of light alkanes with SnO2 nanocrystals: a DFT-based insight. Physical Chemistry Chemical Physics, 2009, 11, 3634.	1.3	10
473	Substrate effects on the structural and photoresponse properties of CVD grown ZnO nanostructures: aluminavs.silica. CrystEngComm, 2011, 13, 656-662.	1.3	10
474	Multicomponent oxide thin-film transistors fabricated by a double-layer inkjet printing process. Thin Solid Films, 2011, 520, 1334-1340.	0.8	10
475	Soft chemistry routes to transparent metal oxide thin films. The case of sol–gel synthesis and structural characterization of Ta2O5 thin films from tantalum chloromethoxide. Thin Solid Films, 2014, 555, 39-41.	0.8	10
476	Section de capture des trous sur le niveau Ev + 0,34 eV de Si : Pt. Revue De Physique Appliquée, 1980, 15, 843-848.	0.4	10
477	High performance silicon electrode enabled by titanicone coating. Scientific Reports, 2022, 12, 137.	1.6	10
478	The influence of cobalt on the electrical characteristics of ZnO ceramics. Materials Science & Engineering A: Structural Materials: Properties, Microstructure and Processing, 1989, 109, 201-205.	2.6	9
479	Initial stage of epitaxial growth at low temperature of GaAs and AlAs on Si by atomic layer molecular beam epitaxy (ALMBE) and MBE. Journal of Crystal Growth, 1992, 123, 385-392.	0.7	9
480	Interface defects and inhomogeneities induced by alloy clustering in InAlAs buffer layers grown on InP. Applied Surface Science, 1993, 65-66, 447-454.	3.1	9
481	Frequencyâ€Resolved Admittance Measurements on InAlAs / InGaAs / InAlAs Singleâ€Quantum Determine the Conduction Band Offset and the Capture Coefficient. Journal of the Electrochemical Society, 1993, 140, 1492-1495.	Wells to 1.3	9
482	Influence of mismatch on the defects in relaxed epitaxial InGaAs/GaAs(100) films grown by molecular beam epitaxy. Journal of Applied Physics, 1993, 74, 1731-1735.	1.1	9
483	Atomic diffusion induced by stress relaxation in InGaAs/GaAs epitaxial layers. Journal of Applied Physics, 1997, 82, 1147-1152.	1.1	9
484	Well surface roughness and fault density effects on the Hall mobility of In[sub x]Ga[sub 1â^'x]As/In[sub y]Al[sub 1â^'y]As/InP high electron mobility transistors. Journal of Vacuum Science & Technology an Official Journal of the American Vacuum Society B, Microelectronics Processing and Phenomena, 1997, 15, 1715.	1.6	9
485	Polycrystalline silicon layers for micromechanical applications: stress profile analysis. Microelectronics Journal, 1997, 28, 433-448.	1.1	9
486	An investigation of the properties of intimate InInxGa1-xAs(100) interfaces formed at room and cryogenic temperatures. Applied Surface Science, 1998, 123-124, 501-507.	3.1	9

#	Article	IF	CITATIONS
487	Surface roughness in InGaAs channels of high electron mobility transistors depending on the growth temperature: Strain induced or due to alloy decomposition. Journal of Applied Physics, 1998, 83, 7537-7541.	1.1	9
488	Ion beam synthesis of polycrystalline SiC on SiO2structures for MEMS applications. Journal of Micromechanics and Microengineering, 2000, 10, 152-156.	1.5	9
489	Ground and first excited states observed in silicon nanocrystals by photocurrent technique. Solid-State Electronics, 2005, 49, 1112-1117.	0.8	9
490	Grain-boundary resistivity versus grain size distribution in three-dimensional polycrystals. Applied Physics Letters, 2006, 88, 141920.	1.5	9
491	Microinductive Signal Conditioning With Resonant Differential Filters: High-Sensitivity Biodetection Applications. IEEE Transactions on Instrumentation and Measurement, 2007, 56, 1590-1595.	2.4	9
492	Development and characterisation of a screen-printed mixed potential gas sensor. Sensors and Actuators B: Chemical, 2007, 130, 561-561.	4.0	9
493	Crystallization Pathways of Multicomponent Oxide Nanocrystals: Critical Role of the Metal Cations Distribution in the Case Study of Metal Ferrites. Crystal Growth and Design, 2010, 10, 5176-5181.	1.4	9
494	Two step, hydrolytic-solvothermal synthesis of redispersible titania nanocrystals and their gas-sensing properties. Journal of Sol-Gel Science and Technology, 2011, 60, 254-259.	1.1	9
495	Characterization of the interface states at A1-GaAs schottky barriers with a thin interface layer. Solid-State Electronics, 1983, 26, 537-538.	0.8	8
496	Conduction mechanisms and temperature dependence of the electroluminescence in ZnO varistors. Semiconductor Science and Technology, 1986, 1, 230-233.	1.0	8
497	Analysis of the nearâ€intrinsic and extrinsic photocapacitance due to the EL2 level in boronâ€implanted GaAs. Journal of Applied Physics, 1986, 60, 1661-1669.	1.1	8
498	Electroluminescence analysis of the structural damage created in systems by Ar ion implantation. Solid-State Electronics, 1996, 39, 355-359.	0.8	8
499	Photosensor and optical waveguide coupling in silicon technology. Sensors and Actuators A: Physical, 1997, 62, 524-528.	2.0	8
500	Optical characterization of thermally oxidized Si1â^'â^'Ge C layers. Thin Solid Films, 2000, 364, 233-238.	0.8	8
501	Microstructural characterisation of CuInS2 polycrystalline films sulfurised by rapid thermal processing. Thin Solid Films, 2001, 387, 219-221.	0.8	8
502	Analysis of the white emission from ion beam synthesised layers by in-depth resolved scanning photoluminescence microscopy. Materials Science and Engineering B: Solid-State Materials for Advanced Technology, 2002, 91-92, 51-54.	1.7	8
503	Multisensor chip for gas concentration monitoring in a flowing gas mixture. Sensors and Actuators B: Chemical, 2005, 107, 688-694.	4.0	8
504	Strategies towards advanced ion track-based biosensors. Radiation Effects and Defects in Solids, 2009, 164, 431-437.	0.4	8

#	Article	IF	CITATIONS
505	Comparison of Hydrogen Sulfide Sensing Characteristics of Individual SnO2 Nanowire and SnO2 Sol-Gel Nanocomposite. Procedia Engineering, 2012, 47, 1398-1401.	1.2	8
506	Spatial mapping of exciton lifetimes in single ZnO nanowires. APL Materials, 2013, 1, .	2.2	8
507	Impact of the structure of Mo(S,Se) ₂ interfacial region in electrodeposited Culn(S,Se) ₂ solar cells. Physica Status Solidi (A) Applications and Materials Science, 2015, 212, 61-66.	0.8	8
508	Multi-layered photocathodes based on Cu2ZnSnSe4 absorber and MoS2 catalyst for the hydrogen evolution reaction. Journal of Materials Chemistry A, 2019, 7, 24320-24327.	5.2	8
509	Structural Influence of the Anode Materials towards Efficient Zn Deposition/Dissolution in Aqueous Zn-Iodide Flow Batteries. Journal of the Electrochemical Society, 2021, 168, 040532.	1.3	8
510	Temperature-Driven Chemical Segregation in Co-Free Li-Rich-Layered Oxides and Its Influence on Electrochemical Performance. Chemistry of Materials, 2022, 34, 3637-3647.	3.2	8
511	Engineering the Interfacial Microenvironment via Surface Hydroxylation to Realize the Clobal Optimization of Electrochemical CO ₂ Reduction. ACS Applied Materials & Interfaces, 2022, 14, 32157-32165.	4.0	8
512	Interpretation of the electron capture by multiphonon emission at native levels in LPE gallium arsenide. Journal of Physics C: Solid State Physics, 1982, 15, L175-L179.	1.5	7
513	Optical and thermal cross-section of interface states from photocapacitance measurements. Solid-State Electronics, 1986, 29, 1195-1203.	0.8	7
514	Optical and electrical properties of a-SixNy:H films prepared by rf plasma using N2+SiH4 gas mixtures. Journal of Non-Crystalline Solids, 1991, 137-138, 895-898.	1.5	7
515	Alloy inhomogeneities in InAlAs strained layers grown by molecularâ€beam epitaxy. Journal of Applied Physics, 1992, 71, 2470-2471.	1.1	7
516	Silicon nitride elaborated by low pressure chemical vapour deposition from Si2H6 and NH3 at low temperature. Materials Science and Engineering B: Solid-State Materials for Advanced Technology, 1993, 17, 185-189.	1.7	7
517	Three-dimensional structures obtained by double diffusion and electrochemical etch stop. Journal of Micromechanics and Microengineering, 1993, 3, 141-142.	1.5	7
518	Quasiperiodic contrast inhomogeneities induced by clusters in the In0.52Al0.48As/InP interface. Applied Physics Letters, 1993, 62, 2265-2267.	1.5	7
519	Structural analysis of buried AlN thin films formed by nitrogen implantation into microelectronics grade aluminium. Nuclear Instruments & Methods in Physics Research B, 1994, 84, 214-217.	0.6	7
520	Raman Characterization of Polycrystalline Silicon: Stress Profile Measurements. Materials Research Society Symposia Proceedings, 1994, 343, 609.	0.1	7
521	Stress gradient and structural properties of atmospheric and reduced pressure deposited polysilicon layers for micromechanical sensors. Sensors and Actuators A: Physical, 1995, 51, 9-12.	2.0	7
522	Structural analysis of InGaAs tensile layers on InP. Materials Science and Technology, 1996, 12, 190-192.	0.8	7

#	Article	IF	CITATIONS
523	Effect of stress and composition on the Raman spectra of etchâ€stop SiGeB layers. Journal of Applied Physics, 1996, 80, 5736-5741.	1.1	7
524	Quantification by optical absorption of the coarse modulation observed by transmission electron microscopy in InGaAs layers grown on InP(100). Semiconductor Science and Technology, 1996, 11, 1310-1316.	1.0	7
525	Morphology of island nuclei in epitaxial GaAs/Si. Materials Letters, 1997, 31, 339-344.	1.3	7
526	Microraman and microhardness study of nitrogen implanted diamond-like carbon films. Carbon, 1998, 36, 791-794.	5.4	7
527	Oxidation of Si[sub 1â^'y]C[sub y] (0â‰9â‰0.02) strained layers grown on Si(001). Journal of Vacuum Science & Technology an Official Journal of the American Vacuum Society B, Microelectronics Processing and Phenomena, 1998, 16, 1757.	1.6	7
528	Noble Metal Nanostructures Synthesized inside Mesoporous Nanotemplate Pores. Electrochemical and Solid-State Letters, 2004, 7, J17.	2.2	7
529	Improved charge injection in Si nanocrystal non-volatile memories. Microelectronics Reliability, 2005, 45, 899-902.	0.9	7
530	Oxide nanocrystals from a low-temperature, self-limiting sol–gel transition in a coordinating environment: Nanocrystal synthesis, processing of gas-sensing devices and application to organic compounds. Sensors and Actuators B: Chemical, 2007, 126, 163-167.	4.0	7
531	Oxide–oxide nanojunctions in coaxial SnO2/TiO2, SnO2/V2O3 and SnO2/(Ti0.5V0.5)2O3 nanowire heterostructures. CrystEngComm, 2013, 15, 4532.	1.3	7
532	Suppression of the NO2 interference by chromium addition in WO3-based ammonia sensors. Investigation of the structural properties and of the related sensing pathways. Sensors and Actuators B: Chemical, 2013, 187, 308-312.	4.0	7
533	Colloidal synthesis and functional properties of quaternary Cu-based semiconductors: Cu2HgGeSe4. Journal of Nanoparticle Research, 2014, 16, 1.	0.8	7
534	Contact resistance stability and cation mixing in a Vulcan-based LiNi _{1/3} Co _{1/3} Mn _{1/3} O ₂ slurry for semi-solid flow batteries. Dalton Transactions, 2021, 50, 6710-6717.	1.6	7
535	Dislocations in GaAs grown by ALMBE on (001) Si. Materials Letters, 1991, 11, 155-160.	1.3	6
536	Frequency resolved admittance spectroscopy measurements on In0.52Al0.48As/InxGa1â^'xAs/In0.52Al0.48As single quantum well structures. Journal of Applied Physics, 1994, 76, 1077-1080.	1.1	6
537	Contrast modulations in InAIAs/InP. Journal of Electronic Materials, 1994, 23, 969-974.	1.0	6
538	Spontaneous Lateral Modulations in InAlAs Buffer Layers Grown by MBE on InP Substrates. Materials Research Society Symposia Proceedings, 1995, 417, 265.	0.1	6
539	Pressure influence on the decay of the photoluminescence in Si nanopowder grown by plasmaâ€enhanced chemical vapor deposition. Applied Physics Letters, 1995, 67, 2830-2832.	1.5	6
540	Strain, alloy composition, and lattice relaxation measured by opticalâ€absorption spectroscopy. Journal of Applied Physics, 1995, 77, 3393-3398.	1.1	6

#	Article	IF	CITATIONS
541	Intrinsic asymmetry between the [011] and [011Ì,,] crystallographic directions in the In0.52Al0.48As/InP matched system. Journal of Vacuum Science & Technology an Official Journal of the American Vacuum Society B, Microelectronics Processing and Phenomena, 1995, 13, 2057.	1.6	6
542	Influence of interface dislocations on surface kinetics during epitaxial growth of InGaAs. Applied Surface Science, 1998, 123-124, 303-307.	3.1	6
543	Growth Monitoring of Cu-Poor Prepared CuInS2 Thin Films. Materials Research Society Symposia Proceedings, 2001, 668, 1.	0.1	6
544	Growth and characterization of shape memory alloy thin films for Si microactuator technologies. Journal of Materials Science: Materials in Electronics, 2001, 12, 323-326.	1.1	6
545	Electrochemical deposition of metal layers and structures for Si-based microsystems. Sensors and Actuators A: Physical, 2002, 99, 41-44.	2.0	6
546	Luminescent properties of Er and Si co-implanted silicates. Optical Materials, 2005, 27, 910-914.	1.7	6
547	Enhanced Heteroâ€Junction Quality and Performance of Kesterite Solar Cells by Aluminum Hydroxide Nanolayers and Efficiency Limitation Revealed by Atomicâ€resolution Scanning Transmission Electron Microscopy. Solar Rrl, 2018, 3, 1800279.	3.1	6
548	Time-dependent response of interface states determined by using differential isothermal transient spectroscopy. Applied Surface Science, 1987, 30, 120-126.	3.1	5
549	Optical characterization of siliconâ€onâ€insulator material obtained by sequential implantation and annealing. Applied Physics Letters, 1990, 57, 2443-2445.	1.5	5
550	Effect of boron implantation on the structure and residual stress of LPCVD polysilicon films. Journal of Micromechanics and Microengineering, 1992, 2, 170-172.	1.5	5
551	Composition modulation and inhomogeneous strain field inInxGa1â^'xAs/InP strained layers. Physical Review B, 1992, 46, 10453-10456.	1.1	5
552	Accurate infrared spectroscopy analysis in back-side damaged silicon wafers. Applied Surface Science, 1993, 63, 236-239.	3.1	5
553	Semi-Insulating Polycrystalline Silicon by Low Pressure Chemical Vapour Deposition from Disilane and Nitrous Oxide. Japanese Journal of Applied Physics, 1995, 34, 4666-4672.	0.8	5
554	On the structural origin of the photoluminescence in silicon powder produced in PECVD processes. Thin Solid Films, 1996, 276, 96-99.	0.8	5
555	<title>Comprehensive study of processing parameters influencing the stress and stress gradient of thick polysilicon layers</title> . , 1997, 3223, 130.		5
556	Breakdown properties of metal/NIDOS SiO2/silicon structures. Microelectronics Reliability, 1999, 39, 187-190.	0.9	5
557	Ultra thin electronics for space applications. , 0, , .		5
558	Computer image HRTEM simulation of catalytic nanoclusters on semiconductor gas sensor materials supports. Materials Science and Engineering B: Solid-State Materials for Advanced Technology, 2002, 91-92, 534-536.	1.7	5

#	Article	IF	CITATIONS
559	FIB based measurements for material characterization on MEMS structures. , 2005, 5766, 60.		5
560	Monolithic Ceramic Technology for Sensing Devices. , 2009, , .		5
561	Real-Time Raman Scattering Analysis of the Electrochemical Growth of CulnSe2 Precursors for Culn(S,Se)2 Solar Cells. Journal of the Electrochemical Society, 2011, 158, H521.	1.3	5
562	Insight into the structural, electrical and photoresponse properties of individual Fe:SrTiO3 nanotubes. Materials Chemistry and Physics, 2013, 141, 9-13.	2.0	5
563	The Ethylhexanoate Route to Metal Oxide Nanocrystals: Synthesis of CoO Nanooctahedra from Coll 2-Ethylhexanoate. European Journal of Inorganic Chemistry, 2016, 2016, 3963-3968.	1.0	5
564	Au–Manganese Oxide Nanostructures by a Plasmaâ€Assisted Process as Electrocatalysts for Oxygen Evolution: A Chemicoâ€Physical Investigation. Advanced Sustainable Systems, 2020, , 2000177.	2.7	5
565	Dual Improvement of <i>β</i> â€MnO ₂ Oxygen Evolution Electrocatalysts via Combined Substrate Control and Surface Engineering. ChemCatChem, 2020, 12, 5984-5992.	1.8	5
566	Dependence of the optical cross section of interface states on the photon energy at Si-SiO2 structures. Surface Science, 1986, 168, 665-671.	0.8	4
567	Dependence of the Defects Present in InAlAs/InP on the Substrate Temperature. Materials Research Society Symposia Proceedings, 1991, 240, 189.	0.1	4
568	Emission kinetic of the slow interface states in Si3N4/In0.53Ga0.47As structures. Applied Physics Letters, 1991, 58, 919-921.	1.5	4
569	Anomalous optical and electrical recovery processes of the photoquenched EL2 defect produced by oxygen and boron ion implantation in gallium arsenide. Journal of Applied Physics, 1992, 71, 252-259.	1.1	4
570	Evolution upward from the interface of the coarse structure existing in inhomogeneous III–V epitaxial layers. Materials Letters, 1992, 13, 47-50.	1.3	4
571	Infrared analysis of buried insulator layers formed by ion implantation into silicon. Applied Surface Science, 1993, 63, 312-315.	3.1	4
572	Anisotropic etch-stop properties of nitrogen-implanted silicon. Sensors and Actuators A: Physical, 1994, 45, 219-225.	2.0	4
573	Pressure dependence of photoluminescence in amorphous silicon nanopowder produced by plasma enhanced chemical vapour deposition. Materials Science and Technology, 1995, 11, 707-710.	0.8	4
574	Partial and perfect dislocation nucleation at the onset of stress relaxation in In0.60Ga0.40As active layers of high mobility transistors grown on InP. Journal of Applied Physics, 1995, 77, 4993-4996.	1.1	4
575	Ion beam assisted recrystallization of structures. Nuclear Instruments & Methods in Physics Research B, 1996, 112, 334-337.	0.6	4
576	Etch‣top Behavior of Buried Layers Formed by Substoichiometric Nitrogen Ion Implantation into Silicon. Journal of the Electrochemical Society, 1996, 143, 1026-1033.	1.3	4

#	Article	IF	CITATIONS
577	Comparative Study of Implanted and Sputtered Systems of Si Nanograins Embedded In SiO ₂ . Materials Research Society Symposia Proceedings, 1997, 486, 225.	0.1	4
578	On the Incorporation of Carbon In SiO ₂ Layers. Defect and Diffusion Forum, 1998, 160-161, 1-24.	0.4	4
579	Influence of Deposit Thickness on the Microstructure and Surface Roughness of Silicon Films Deposited from Silane. Solid State Phenomena, 1999, 67-68, 125-130.	0.3	4
580	Charge Storage Effects in Si Nanocrystals Embedded in SiO ₂ Thin Films. Solid State Phenomena, 2001, 80-81, 243-248.	0.3	4
581	New Tunnel Schottky SiC Devices Using Mixed Conduction Ceramics. Materials Science Forum, 2003, 433-436, 949-952.	0.3	4
582	HRTEM/EELS Analysis, Structural Characterization and Sensor Performances of Hydrothermal Nano-TiO ₂ . Materials Research Society Symposia Proceedings, 2004, 828, 155.	0.1	4
583	Electrical Contacts and Gas Sensing Analysis of Individual Metal Oxide Nanowires and 3-D Nanocrystal Networks. IEEJ Transactions on Sensors and Micromachines, 2006, 126, 537-547.	0.0	4
584	Morphological and structural characterization of WO3 and Cr–WO3 thin films synthesized by sol–gel process. Thin Solid Films, 2010, 518, 4512-4514.	0.8	4
585	Stress gradient and structural properties of atmospheric and reduced pressure deposited polysilicon layers for micromechanical sensors. , 1995, 51, 9-9.		4
586	Poole Frenkel Effect on the DX Centers in III-V Ternary Alloys. Materials Research Society Symposia Proceedings, 1989, 163, 785.	0.1	3
587	Percolation Behaviour in the Electrical Characteristics of Hydrogenated Amorphous Silicon Nitride Films Materials Research Society Symposia Proceedings, 1992, 258, 655.	0.1	3
588	Buried oxide layers formed by oxygen implantation on screened oxide silicon wafers: structural analysis. Nuclear Instruments & Methods in Physics Research B, 1993, 80-81, 838-841.	0.6	3
589	Structural characterisation of nitrogen ion implantation into silicon for sensor technology. Nuclear Instruments & Methods in Physics Research B, 1993, 80-81, 702-705.	0.6	3
590	Optical characterisation of SIMOX structures formed by successive implantation and annealing. Nuclear Instruments & Methods in Physics Research B, 1994, 84, 275-280.	0.6	3
591	Optimization of voltage-controlled thin-film microstructures. Sensors and Actuators A: Physical, 1995, 47, 613-617.	2.0	3
592	Structural Analysis of Nanocrystals Embedded in Amorphous Si Films. Materials Research Society Symposia Proceedings, 1996, 452, 785.	0.1	3
593	Gas collisions and pressure quenching of the photoluminescence of silicon nanopowder grown by plasma-enhanced chemical vapor deposition. Journal of Applied Physics, 1997, 81, 3290-3293.	1.1	3
594	TEM characterisation of high pressure–high-temperature-treated Czochralski silicon samples. Materials Science and Engineering B: Solid-State Materials for Advanced Technology, 2000, 73, 250-254.	1.7	3

#	Article	IF	CITATIONS
595	Epitaxial Growth of β-SiC on Ion-Beam Synthesized β-SiC: Structural Characterization. Materials Science Forum, 2000, 338-342, 309-312.	0.3	3
596	<title>Low-cost thermal flow sensor for home-appliances applications</title> ., 2002, , .		3
597	TEM 3D Tomography of Noble Metal Nanowires Growth Inside SiO2 Mesoporous Aggregates. Materials Research Society Symposia Proceedings, 2004, 818, 239.	0.1	3
598	Impact of carbon concentration on the interface density of states of metal-oxide Si1â^'xâ^'y GexCy (strained) capacitors. Journal of Electronic Materials, 2004, 33, 1022-1027.	1.0	3
599	Novel design and preliminary results of YSZ electrolyte-based amperometric oxygen sensors. , 0, , .		3
600	Solid Electrolyte Multisensor System for Detecting O[sub 2], CO, and NO[sub 2]. Journal of the Electrochemical Society, 2007, 154, J201.	1.3	3
601	Ultimate response dynamics achieved with gas sensors based on self-heated nanowires. Procedia Chemistry, 2009, 1, 1427-1430.	0.7	3
602	Retrieving the spatial distribution of cavity modes in dielectric resonators by near-field imaging and electrodynamics simulations. Nanoscale, 2012, 4, 1620.	2.8	3
603	Towards Production of a Highly Catalytic and Stable Graphene-Wrapped Graphite Felt Electrode for Vanadium Redox Flow Batteries. Batteries, 2018, 4, 63.	2.1	3
604	2Dâ€Organic Layered Materials: Atomically dispersed Fe in a C ₂ N Based Catalyst as a Sulfur Host for Efficient Lithium–Sulfur Batteries (Adv. Energy Mater. 5/2021). Advanced Energy Materials, 2021, 11, 2170022.	10.2	3
605	Study of Lanthanum compounds influence on tin oxide CO2 gas sensors. , 2003, , .		3
606	Analysis of the edge region photocapacitance at constant bias in Te-doped Al0.55Ga0.45As. Solid-State Electronics, 1986, 29, 759-766.	0.8	2
607	Optical Isothermal Transient Spectroscopy: Application to the Boron Implantation in GaAs. Materials Science Forum, 1986, 10-12, 539-544.	0.3	2
608	TEM techniques for two dimensional junction delineation in integrated circuits. Micron and Microscopica Acta, 1989, 20, 151-152.	0.2	2
609	Raman scattering and photoluminescence analysis of SOI/SIMOX structures obtained by sequential implantation and annealing correlated with cross sectional TEM. Nuclear Instruments & Methods in Physics Research B, 1991, 55, 714-717.	0.6	2
610	Correlation Between Electrical and Structural Characterization of In0.53Ga0.47As / Si3 N 4 Inte on MIS Structures. Journal of the Electrochemical Society, 1991, 138, 3470-3473.	erfaçes 1.3	2
611	Electroluminescence Evaluation of the SiO ₂ -Si Structures Using an Electrolyte-SiO ₂ -Si Cell. Materials Research Society Symposia Proceedings, 1993, 298, 253.	0.1	2
612	Ion beam synthesis of aluminium nitride: characterisation of thin AIN layers formed in microelectronics aluminium. Materials Science and Technology, 1995, 11, 1187-1190.	0.8	2

#	Article	IF	CITATIONS
613	Structural analysis of thermally oxidized amorphous Si1-xGex layers. Microelectronic Engineering, 1995, 28, 225-228.	1.1	2
614	Analysis by optical absorption and transmission electron microscopy of the strain inhomogeneities in InGaAs/InP strained layers. Journal of Applied Physics, 1995, 77, 4018-4020.	1.1	2
615	Electron capture and emission by the Ti acceptor level in GaP. Journal of Applied Physics, 1995, 78, 2441-2446.	1.1	2
616	Composition inhomogeneities in the buffer layers of In0.52Al0.48As/InxGa1â^'xAs/InP multiquantum well structures driven by In segregation. Journal of Vacuum Science & Technology an Official Journal of the American Vacuum Society B, Microelectronics Processing and Phenomena, 1995, 13, 1006.	1.6	2
617	Ion beam synthesis and recrystallization of amorphous SiGe/SiC structures. Nuclear Instruments & Methods in Physics Research B, 1996, 120, 151-155.	0.6	2
618	High temperature high dose C ion implantation in epitaxial SiGe. Nuclear Instruments & Methods in Physics Research B, 1996, 120, 173-176.	0.6	2
619	Influence of the Technological Parameters on the Mechanical Properties of Thick Epipolysilicon Layers for Micromechanical Sensors. Solid State Phenomena, 1996, 51-52, 423-428.	0.3	2
620	Microstructure Influence on the First Stage of the Oxidation Process in Polycrystalline SiGe Layers. Solid State Phenomena, 1996, 51-52, 199-204.	0.3	2
621	Growth Control And Characterization Of Wide Band Gap Silicon-Carbon Films. Materials Research Society Symposia Proceedings, 1997, 483, 247.	0.1	2
622	Blue, Yellow-Green and Red Simultaneous Emission from SiO ₂ Matrices Co-Implanted with Si and C. Materials Research Society Symposia Proceedings, 1997, 486, 237.	0.1	2
623	Correlation of electrical anisotropies of HEMT devices with defect distribution and InGaAs well roughness. Materials Science and Engineering B: Solid-State Materials for Advanced Technology, 1997, 44, 325-329.	1.7	2
624	Structure and photoluminescence of annealed semi-insulating polycrystalline silicon material obtained by disilane. Thin Solid Films, 1997, 296, 98-101.	0.8	2
625	Ultra low energy SIMS, XTEM and X-ray diffraction methods for the characterization of a MBE grown short period (Si Ge)16 superlattices. Thin Solid Films, 2000, 367, 176-179.	0.8	2
626	Ion beam synthesis of n-type doped SiC layers. Applied Surface Science, 2001, 184, 367-371.	3.1	2
627	Evaluation of sensitive materials for integrated thermal flow sensors. , 0, , .		2
628	Ultra-thinned chips integration: technological approach and electrical qualification. , 0, , .		2
629	Luminescence and Morphological Properties of GaN Layers Grown on SiC/Si(111) Substrates. Physica Status Solidi A, 2002, 192, 401-406.	1.7	2
630	Transmission electron microscopy and image simulation study of CuAu domains in CuInS2 epitaxial layers. Thin Solid Films, 2003, 431-432, 226-230.	0.8	2

#	Article	IF	CITATIONS
631	Precipitation of highly luminescent phases from PECVD Si suboxides. Materials Research Society Symposia Proceedings, 2004, 832, 303.	0.1	2
632	Optimized screen-printing and SEM-FIB characterization of YSZ thin films for Solid Oxide Fuel Cells and gas sensors devices. Materials Research Society Symposia Proceedings, 2004, 822, S6.11.1.	0.1	2
633	Low loss silica waveguides containing Si nanocrystals. Materials Research Society Symposia Proceedings, 2004, 817, 80.	0.1	2
634	Optical and electrical properties of Si1â^'xâ^'yGexCy strained layers thermally oxidized. Microelectronic Engineering, 2004, 72, 185-190.	1.1	2
635	Crystalline mesoporous tungsten oxide for gas sensing applications. , 0, , .		2
636	Microcoils for biosensors fabricated by focused ion beam (FIB). , 0, , .		2
637	Micro and nanotechnologies for the development of an integrated chromatographic system. , 2007, , .		2
638	Linear and non linear behavior of mechanical resonators for optimized inertial electromagnetic microgenerators. , 2008, , .		2
639	Room temperature conductometric gas sensors based on metal oxide nanowires and nanocrystals. , 2009, , .		2
640	Characterisation of Secondary Phases in Cu Poor CuInSe2: Surface and in-depth resolved Raman scattering analysis of polycrystalline layers. Materials Research Society Symposia Proceedings, 2009, 1165, 1.	0.1	2
641	Nanoporous films obtained by sacrificial layer pulsed laser deposition. Thin Solid Films, 2009, 518, 383-386.	0.8	2
642	Individual nanowire chemical sensor system self-powered with energy scavenging technologies. , 2009, , .		2
643	Luminescence studies of isolated ZnO nanowires grown by the vapourâ€liquidâ€solid method. Physica Status Solidi C: Current Topics in Solid State Physics, 2012, 9, 1537-1539.	0.8	2
644	SoH evaluation of LiFePO <inf>4</inf> cells using impedance and thermal measurements. , 2014, , .		2
645	Solvothermal Synthesis, Gasâ€Sensing Properties, and Solar Cellâ€Aided Investigation of TiO ₂ –MoO _x Nanocrystals. ChemNanoMat, 2017, 3, 798-807.	1.5	2
646	Role of milling parameters on the mechano-chemically synthesized mesoporous nanosilicon properties for Li-ion batteries anode. Journal of Physics and Chemistry of Solids, 2020, 139, 109318.	1.9	2
647	Acidic and Basic Sites in Iron Modified Nano-TiO ₂ for Gas Sensors. Sensor Letters, 2008, 6, 1041-1044.	0.4	2
648	Modification of the Silicon Surface by Electroless Deposition of Platinum from HF Solutions. Materials Research Society Symposia Proceedings, 1996, 451, 275.	0.1	2

#	Article	IF	CITATIONS
649	Negative capacitance in switching MISS devices. Physica B: Physics of Condensed Matter & C: Atomic, Molecular and Plasma Physics, Optics, 1985, 129, 351-355.	0.9	1
650	Optical Assessment of the Interaction Between EL2 and EL6 Levels in Boron Implanted GaAs. Physica Scripta, 1987, 35, 524-527.	1.2	1
651	Effects of surface plasma treatments in relation to electrical isolation in GaAs integrated circuits. Surface Science, 1991, 251-252, 195-199.	0.8	1
652	On the capacitance control in deep level spectroscopy. Measurement Science and Technology, 1991, 2, 899-906.	1.4	1
653	TEM Studies of Alloy Clustering in InAlAs Strained Layers. Materials Research Society Symposia Proceedings, 1991, 240, 111.	0.1	1
654	Complete identification of the Ti-related levels in GaP. Applied Surface Science, 1991, 50, 496-499.	3.1	1
655	Influence of the Cobalt on the Electroluminescence Spectra of ZnO. Materials Science Forum, 1991, 38-41, 567-572.	0.3	1
656	Electrical Evaluation of Silicon on Insulator Structures Formed by Oxygen Implantation by Means of Frequency Resolved Photoconductivity Measurements. Solid State Phenomena, 1991, 19-20, 511-516.	0.3	1
657	TEM Techniques for 2D Junction Delineation and Correlation with SIMS and SRP. Solid State Phenomena, 1991, 19-20, 449-454.	0.3	1
658	Composition Modulation Effects on the Generation of Defects in In _{0.54} Ga _{0.46} As Strained Layers. Materials Science Forum, 1992, 83-87, 1285-1290.	0.3	1
659	HF/Ethanol Preoxidation Silicon Cleaning: Analysis of the Silicon Surface and of the Ultra-Thin Oxide Layer. Materials Research Society Symposia Proceedings, 1992, 259, 119.	0.1	1
660	Tem Study of Temperature Influence on The Crystalline Quality of InGaAs/Si Epilayers. Materials Research Society Symposia Proceedings, 1992, 263, 503.	0.1	1
661	Materials problems for the development of InGaAs/InAlAs HEMT technology. Materials Science and Engineering B: Solid-State Materials for Advanced Technology, 1993, 20, 21-25.	1.7	1
662	Analysis of the SiO2 defects originated by phosphorus implantation in MOS structures. Nuclear Instruments & Methods in Physics Research B, 1993, 80-81, 612-615.	0.6	1
663	Morphological characterization of InAlAs/InAs and InAlAs/InGaAs multiple-quantum-well structures grown on InP substrates. Materials Letters, 1993, 15, 363-369.	1.3	1
664	Passivation analysis of (100) surfaces by anodic oxidation in aqueous KOH. Journal of Micromechanics and Microengineering, 1993, 3, 138-140.	1.5	1
665	Microstructure of Buried Thin Etch Stop Films Formed by Nitrogen Implantation into Silicon. Materials Research Society Symposia Proceedings, 1993, 308, 361.	0.1	1
666	Stacking Fault-Like Fringes Along <010> Directions Observed in In0.52Al0.48 as Layers on the (100) Zone Axis. Materials Research Society Symposia Proceedings, 1993, 312, 131.	0.1	1

#	Article	IF	CITATIONS
667	Analysis of the HF-Etihanol Cleaning Process on Silicon Wafers with 100 Vicinal Surfaces. Materials Research Society Symposia Proceedings, 1993, 315, 473.	0.1	1
668	IR-Visible Photoluminescence Study of Nanometer-Size Amorphous Silicon Powder Produced by Square-Wave-Modulated RF Glow Discharge. Materials Research Society Symposia Proceedings, 1994, 351, 405.	0.1	1
669	On The Origin of The Coarse and Fine Contrast Modulation in Epitaxial InGaAs Strained Layers Grown On InP Substrates Materials Research Society Symposia Proceedings, 1995, 379, 159.	0.1	1
670	Synthesis of Thin Membranes in Si Technology by Carbon Ion Implantation. Materials Research Society Symposia Proceedings, 1995, 396, 727.	0.1	1
671	Raman scattering analysis of SiGe annealed and implanted layers. , 0, , .		1
672	Electrostatically controlled multi-purpose torsional structures obtained on monocrystalline silicon. Journal of Micromechanics and Microengineering, 1996, 6, 103-104.	1.5	1
673	Structural Changes on SnO2 Nanoparticles for Gas Sensor Applications induced by Calcination Treatments and Grinding. Materials Research Society Symposia Proceedings, 1997, 501, 53.	0.1	1
674	Ion beam synthesis of SiC in silicon-on-insulator. , 0, , .		1
675	Investigation of roughness and defect nucleation anisotropies on tensile InxGa1 â^' xAs/In(P001). Materials Letters, 1997, 32, 103-107.	1.3	1
676	Structural characterization of InGaAs/InAlAs quantum wells grown on 0 (111)-InP substrates. Microelectronics Journal, 1997, 28, 999-1003.	1.1	1
677	Phase stepping microscopy for layer thickness measurement in silicon-on-insulator structures. Thin Solid Films, 1997, 311, 225-229.	0.8	1
678	Structural analysis of buried conducting CoSi2 layers formed in Si by high-dose Co ion implantation. Journal of Crystal Growth, 1998, 187, 435-443.	0.7	1
679	Morphology evolution of InSb island grown on InP substrates by atomic layer molecular beam epitaxy. Microelectronic Engineering, 1998, 43-44, 51-57.	1.1	1
680	Atomistic simulations of the Ostwald ripening of Si nanoparticles ion beam synthesized in SiO2. Materials Research Society Symposia Proceedings, 2000, 647, 1.	0.1	1
681	Hole traps and charges in ion implanted MOS capacitors: sensitivity to ionizing radiation. Microelectronics Reliability, 2000, 40, 803-806.	0.9	1
682	<title>Thermal-induced stress in dielectric membranes suitable for micromechanized gas
sensors</title> . , 2001, 4408, 81.		1
683	Mechanical Properties of Thin and Thick Polysilicon Films for Microsystem Applications. Solid State Phenomena, 2001, 80-81, 405-416.	0.3	1
684	Title is missing!. Sensors and Actuators A: Physical, 2002, 99, 1-2.	2.0	1

#	Article	IF	CITATIONS
685	BaSnO/sub 3/ oxygen sensors without the need of a reference electrode. , 0, , .		1
686	Si1-xGex Nanocrystals Observed by EFTEM: Influence of the Dry and Wet Oxidation Process. Materials Research Society Symposia Proceedings, 2004, 832, 158.	0.1	1
687	Chemical Synthesis, Characterization and Gas-Sensing Properties of Thin Films in the In2O3-SnO2 System. Materials Research Society Symposia Proceedings, 2004, 828, 209.	0.1	1
688	Location of Er atoms with respect to Si nanoclusters in luminescent Er and Si co-implanted silicates. Materials Research Society Symposia Proceedings, 2004, 832, 105.	0.1	1
689	Fe2O3:SnO2 Nanostructured System as Semiconductor Gas Sensor Material. Materials Research Society Symposia Proceedings, 2004, 828, 215.	0.1	1
690	Low Voltage and High Speed Silicon Nanocrystal Memories. Materials Research Society Symposia Proceedings, 2004, 830, 78.	0.1	1
691	<title>3D deformation analysis of flow and gas sensors membranes for reliability assessment</title> . , 2005, , .		1
692	Thermal oxidation of Si[sub 1â^'xâ^'y]Ge[sub x]C[sub y] epitaxial layers characterized by Raman and infrared spectroscopies. Journal of Vacuum Science & Technology an Official Journal of the American Vacuum Society B, Microelectronics Processing and Phenomena, 2005, 23, 5.	1.6	1
693	HRTEM and XRD analysis of P6mm and Ia3d double gyroidal WO3 structures. , 2005, , 333-336.		1
694	Fabrication of Electrical Nanocontacts to Nanometer-sized materials and Structures Using a Focused Ion Beam. Materials Research Society Symposia Proceedings, 2005, 872, 1.	0.1	1
695	Design and implementation of mechanical resonators for optimized inertial electromagnetic microgenerators. , 2007, , .		1
696	Electrodeposited CuIn(S, Se)2 films for low cost high efficiency solar cell applications: microstructural analysis. , 2007, , .		1
697	Applications of atomistic calculations to chemical gas sensing. , 2008, , .		1
698	The role of oxygen vacancies in the sensing properties of SnO <inf>2</inf> nanocrystals. , 2008, , .		1
699	Photoexcited Individual Nanowires: Key Elements in Room Temperature Detection of Oxidizing Gases. , 2009, , .		1
700	Simultaneous CO and Humidity Quantification with Self-Heated Nanowires in Pulsed Mode. Procedia Engineering, 2011, 25, 1485-1488.	1.2	1
701	Mesoporous ceria-zirconia solid solutions as oxygen gas sensing material using high temperature hot plates. , 2012, , .		1
702	Photochemical activity of TiO2nanotubes. , 2013, , .		1

Photochemical activity of TiO2nanotubes. , 2013, , . 702

#	Article	IF	CITATIONS
703	Highly efficient surface ionization gas detectors using microfabricated platforms with integrated surface electrodes. , 2013, , .		1
704	Implementation of Multijunction Solar Cells in Integrated Devices for the Generation of Solar Fuels. , 2018, , 349-384.		1
705	Photoelectrochemical Water Splitting: Boosting Photoelectrochemical Water Oxidation of Hematite in Acidic Electrolytes by Surface State Modification (Adv. Energy Mater. 34/2019). Advanced Energy Materials, 2019, 9, 1970131.	10.2	1
706	Microstructure of Pyramidal Defects in InSb Layers Grown by Atomic Layer Molecular Beam Epitaxy on InP Substrates. Journal De Physique III, 1997, 7, 2317-2324.	0.3	1
707	Anisotropic distribution of crystalline defects along [011] and [011] directions in In _{0.52} AI _{0.48} As buffer layers grown on InP. Materials Science and Technology, 1997, 13, 957-960.	0.8	1
708	Boosting Photoelectrochemical Water Oxidation of Hematite by Surface States Modification. SSRN Electronic Journal, 0, , .	0.4	1
709	SnO ₂ nanocristalino mediante pirólisis lÃquida. Boletin De La Sociedad Espanola De Ceramica Y Vidrio, 2000, 39, 560-563.	0.9	1
710	SiCOI Structures. Technology and Characterization. , 2002, , 17-29.		1
711	Optical And Electrical Characteristics Of Leds Fabricated From Si-Nanocrystals Embedded In Sio2. , 2003, , 45-54.		1
712	Evolución de la morfologÃa y facetaje de nanoestructuras de SnO ₂ crecidas por pirólisis en fase aerosol sobre sustratos de vidrio. Boletin De La Sociedad Espanola De Ceramica Y Vidrio, 2004, 43, 510-513.	0.9	1
713	Nanocristales de silicio en matriz de SiO ₂ para aplicaciones fotónicas. Boletin De La Sociedad Espanola De Ceramica Y Vidrio, 2004, 43, 390-393.	0.9	1
714	Nanosensors: Controlling Transduction Mechanisms at the Nanoscale Using Metal Oxides and Semiconductors. , 2009, , 1-51.		1
715	Reply to comment on "characterization of the interface states at Alî—,GaAs Schottky barriers with a thin interface layerâ€: Solid-State Electronics, 1984, 27, 1157.	0.8	Ο
716	Analysis of the capacitance of CdS/CuInSe2 thin film heterojunctions. Thin Solid Films, 1985, 125, 107-112.	0.8	0
717	Hopping Process in Majority Carrier Capture of Deep Centers in Semiconductors. Physica Scripta, 1987, 35, 717-720.	1.2	0
718	Boron implantation influence on the backgating effect in GaAs MESFETs. Vacuum, 1987, 37, 411-413.	1.6	0
719	Boron implantation effects on Au: GaAs Schottky barrier. Vacuum, 1987, 37, 415-417.	1.6	0
720	Isolation quality in passivated semi-insulating GaAs analyzed by leakage current transients. Applied Surface Science, 1989, 39, 144-150.	3.1	0

#	Article	IF	CITATIONS
721	Influence of the surface treatments by multipolar plasma on the slow state tunnel kinetics at the In0.53Ga0.47As/Si3N4 interfaces. Surface Science, 1991, 251-252, 115-118.	0.8	0
722	Raman Microprobe Analysis of Simox Structures Implanted With Screen Oxide. Materials Research Society Symposia Proceedings, 1991, 235, 121.	0.1	0
723	Influence of The Growth Temperature on The Presence of Composition Inhomogeneities in In0.52Al0.48As Layers Grown by MBE on InP Substrates. Materials Research Society Symposia Proceedings, 1992, 263, 101.	0.1	0
724	Near Bandgap Optical Absorption Measurements on InGaAs/InP Strained Layers with Coarse Structure. Materials Research Society Symposia Proceedings, 1992, 263, 353.	0.1	0
725	Tem Assessment of Different Mechanisms Contributing to Stress Relaxation in Strained InGaAs/InAlAs Systems. Materials Research Society Symposia Proceedings, 1992, 263, 467.	0.1	0
726	Raman Spectroscopy Analysis of Nitrogen Ion Implantation in Silicon and Correlation with Transmission Electron Microscopy. Materials Research Society Symposia Proceedings, 1992, 279, 177.	0.1	0
727	Effects of electric field on photoconductive frequency resolved spectroscopy: Analysis of silicon-on-insulator structures. Solid-State Electronics, 1992, 35, 1337-1342.	0.8	0
728	Relation between electrical conductivity and structural characteristics in boron-doped LPCVD polycrystalline silicon used in sensor devices. Sensors and Actuators A: Physical, 1993, 37-38, 68-73.	2.0	0
729	Electrical Characterization of Passivation Processes in Si-GaAs by Isothermal Photoinduced Transient Measurements. Materials Research Society Symposia Proceedings, 1993, 300, 501.	0.1	0
730	Characterization of the Degradation Processes in SiO2-Si Structure by Means of Electrolyte-Insulating-Semiconductor Systems. Materials Research Society Symposia Proceedings, 1993, 309, 49.	0.1	0
731	Analysis of Structural Transformations in High Fluence Nitrogen Ion Implanted Aluminium. Materials Research Society Symposia Proceedings, 1993, 311, 191.	0.1	0
732	The characteristics of intimate Auî—,InyAl1 â^' yAs Schottky diodes: a mismatch dependence study. Materials Science and Engineering B: Solid-State Materials for Advanced Technology, 1994, 28, 433-438.	1.7	0
733	TEM analysis of InGaAs/InAlAs epitaxial layers grown over InP patterned substrates. Materials Letters, 1994, 21, 371-375.	1.3	0
734	Structural Characterization of InAlAs/InGaAs Layers Grown on InP Patterned Substrates. Materials Research Society Symposia Proceedings, 1994, 340, 59.	0.1	0
735	Effect of the Introduction of a MBE Buffer Layer on the Morphology of InSb Almbe Layers Grown on InP Substrates. Materials Research Society Symposia Proceedings, 1995, 399, 473.	0.1	0
736	First Stages of the Platinum Electroless Deposition on Silicon (100) from Hf Solutions Materials Research Society Symposia Proceedings, 1995, 402, 611.	0.1	0
737	Silicon Recrystallization in Sipos Material Obtained by Disilane. Materials Research Society Symposia Proceedings, 1995, 403, 351.	0.1	0
738	Annealing effects in undoped and phosphorus doped low temperature oxide layers. Materials Science and Technology, 1995, 11, 1219-1222.	0.8	0

Joan R Morante

#	Article	IF	CITATIONS
739	Transfer function determination of micromechanical structures using a time domain analysis and resonance method. Sensors and Actuators A: Physical, 1995, 46, 58-61.	2.0	0
740	Modified interferential method for locating coaxial cable faults. , 0, , .		0
741	Local structure and oxygen absorption in a-Si _{1â^'x} C _x (<i>x</i> < 0·4) alloys grown on silicon by plasma enhanced chemical vapour deposition. Materials Science and Technology, 1996, 12, 103-107.	0.8	0
742	Morphological analysis of nanocrystalline SnO2 for gas sensor applications. , 1996, , 1-8.		0
743	Structural Studies of Annealing Effects on Semi-Insulating Polycrystalline Layers Obtained by Using Disilane. Solid State Phenomena, 1996, 51-52, 155-160.	0.3	Ο
744	Raman Scattering Analysis of Defects in 6H-SiC Induced by Ion Implantation. Materials Science Forum, 1997, 258-263, 727-732.	0.3	0
745	Defects Analysis in Strained InAlAs and InGaAs Films Grown on (111)B InP Substrates. Materials Science Forum, 1997, 258-263, 1211-1216.	0.3	0
746	Comparison between AS-Grown and Annealed Quantum Dots Morphology. Materials Science Forum, 1997, 258-263, 1689-1694.	0.3	0
747	Anisotropic distribution of crystalline defects along [011] and [011] directions in In _{0.52} AI _{0.48} As buffer layers grown on InP. Materials Science and Technology, 1997, 13, 957-960.	0.8	0
748	Damage behaviour and annealing of germanium implanted 6H-SiC. , 0, , .		0
749	Self-organization of quantum wire-like morphology on InxGa1 â^ xAs single quantum wells grown on (100)InP vicinal surfaces depending on the substrate misorientation, buffer mismatch and growth temperature. Microelectronics Journal, 1997, 28, 865-873.	1.1	0
750	Diagnostics of nitrogen-implanted diamond-like carbon films by optical and microhardness measurements. , 1998, 3359, 339.		0
751	Optical characterization of carbon ion implantation into Si and SiGe alloys. , 1998, 3359, 324.		Ο
752	Phase Segregation in Sipos: Formation of Si Nanocrystals. Materials Research Society Symposia Proceedings, 1998, 536, 481.	0.1	0
753	Structure Dependence of the Electrical Conductivity of Hydrogenated Nanocrystalline Silicon Films. Solid State Phenomena, 1999, 67-68, 143-148.	0.3	Ο
754	Cubic Silicon Carbide Films Grown by Reactive Magnetron Sputtering at Relatively Low Temperature. Solid State Phenomena, 1999, 67-68, 477-484.	0.3	0
755	Comparison of homogeneously grown and temperature-graded InAlAs buffers in the range 400–560°C: effects on surface morphology and layer stability. Thin Solid Films, 1999, 357, 61-65.	0.8	0
756	Correlation between Structural and Optical Properties of Si Nanocrystals in SiO2: Model for the Visible Light Emission. Materials Research Society Symposia Proceedings, 2000, 647, 1.	0.1	0

#	Article	IF	CITATIONS
757	Correlation between Structural and Optical Properties of Si Nanocrystals in SiO2: Model for the Visible Light Emission. Materials Research Society Symposia Proceedings, 2000, 650, 1351.	0.1	0
758	Influence of Thermal Treatments on the Crystallisation of LPCVD-Deposited Si Thin Films. Solid State Phenomena, 2001, 80-81, 199-204.	0.3	0
759	Structural and Electrical Characterization of Ion Beam Synthesized and n-Doped SiC Layers. Materials Science Forum, 2001, 353-356, 591-594.	0.3	0
760	Induced Pd nanoclustering on SnO/sub 2/ nanoparticles for the enhancement of gas sensor devices. , 0, , .		0
761	Integrated inductances for Si-technology based high sensitivity biosensors. , 0, , .		0
762	Integrated micromachined gas multisensor for domestic boilers. , 0, , .		0
763	Electrical qualification of new ultrathin integration techniques. Microelectronics Reliability, 2003, 43, 111-115.	0.9	0
764	Compatibility of gas and flow sensor technology fabrication. , 2003, , .		0
765	Optical properties of silicates co-doped with Si and Er3+ ions. Materials Research Society Symposia Proceedings, 2004, 832, 81.	0.1	0
766	Reliable, Fast and Long Retention Si Nanocrystal Non-Volatile Memories. Materials Research Society Symposia Proceedings, 2004, 830, 231.	0.1	0
767	Pump-probe experiments on low loss silica waveguides containing Si nanocrystals. Materials Research Society Symposia Proceedings, 2004, 832, 33.	0.1	0
768	Conductivity dependence on oxygen partial pressure and transport number measurements of La2Mo2O9. Materials Research Society Symposia Proceedings, 2004, 822, S6.5.1.	0.1	0
769	Nanostructured mesoporous tungsten oxide for gas sensor applications. , 2005, , .		0
770	Tin and Indium Oxide Nanocrystals Based Gas Sensors Characterization. , 0, , .		0
771	Electrical characterisation of nanowires and nanoparticles contacted using a FIB. , 0, , .		0
772	Design of a microinductive device integrated within a simple resonant diferential filter for high sensitivity portable biodetectors. , 0, , .		0
773	Rib waveguides containing Si nanocrystals embedded in SiO/sub 2/ for optical communication in the visible range. , 0, , .		0
774	Organization of oxygen vacancies in low-temperature La/sub 2/Mo/sub 2/O/sub 9/ ion conductor. , 0, , .		0

#	Article	IF	CITATIONS
775	Electrical response of MOSiC gas sensors to CO, NO/sub 2/ and C/sub 3/H/sub 8/. , 0, , .		Ο
776	Simulation of the influence of particle size distribution and grain boundary resistance on the electrical response of 2D polycrystals. , 0, , .		0
777	Non-nernstian planar YSZ-based electrochenical sensors using semiconducting oxide electrodes. , 0, , .		0
778	Work Function as a Useful Feature for Development of SnO2 Nanowires Based Gas Sensing Devices. , 2006, , .		0
779	Mesostructured WO3 as a sensing material for NO2 detection. Materials Research Society Symposia Proceedings, 2006, 915, 1.	0.1	0
780	Fabrication of bottom-up gas sensors based on individual SnO ₂ nanowires and suspended microhotplates. , 2007, , .		0
781	Nano and micro stripe based metal oxide thin film gas sensor. , 2007, , .		Ο
782	Bottom-up Fabrication of Individual SnO2 Nanowires-based Gas Sensors on Suspended Micromembranes. Materials Research Society Symposia Proceedings, 2007, 1052, 1.	0.1	0
783	A Versatile and Lowâ€Toxicity Route for the Production of Electroceramic Oxide Nanopowders. European Journal of Inorganic Chemistry, 2008, 2008, 954-960.	1.0	Ο
784	Leakage currents and dielectric breakdown of Si1â^'xâ^'yGexCy thermal oxides. Microelectronics Reliability, 2008, 48, 1635-1640.	0.9	0
785	Transparent Oxide Semiconductors Obtained by PLD. Materials Research Society Symposia Proceedings, 2008, 1074, 1.	0.1	Ο
786	Shrinkage Effects of the Conduction Zone in the Electrical Properties of Metal Oxide Nanocrystals: The Basis for Room Temperature Conductometric Gas Sensor. Journal of Sensors, 2009, 2009, 1-6.	0.6	0
787	(S)TEM tomography of AlAs-GaAs coaxial Nanowires. , 2009, , .		Ο
788	Raman scattering based strategies for quality control and process monitoring in electrodeposited CuIn(S,Se)2 solar cell technologies. Materials Research Society Symposia Proceedings, 2009, 1165, 1.	0.1	0
789	Self-Heating in Individual Nanowires: a Major Breakthrough in Sensors Technology. , 2009, , .		0
790	Design and fabrication of Si technology miicrogenerators for vibrational energy scavenging. , 2009, , .		0
791	GaN/AlN Axial Multi Quantum Well Nanowires for Optoelectronic Devices. , 2009, , .		0
792	UV photosensors based on individual semiconductor nanowires. , 2009, , .		0

Joan R Morante

#	Article	lF	CITATIONS
793	Sm0.5Sr0.5CoO3 Electrodes Fabricated at Intermediate Temperatures. ECS Transactions, 2010, 28, 71-79.	0.3	ο
794	Simultaneous Resistive and Ionization Readout of Single Metal Oxide Nanowires. Procedia Engineering, 2011, 25, 1489-1492.	1.2	0
795	Single Material Band Gap Engineering in GaAs Nanowires. , 2011, , .		0
796	Size-dependent recombination dynamics in ZnO nanowires. , 2011, , .		0
797	Multigas sensor based on micro machined hotplates for CO and O <inf>2</inf> detection using catalytically modified nano-SnO <inf>2</inf> . , 2012, , .		0
798	Metal oxides as functional semiconductors. An inkjet approach. Materials Research Society Symposia Proceedings, 2013, 1552, 45-50.	0.1	0
799	Surface modification, heterojunctions, and other structures: composing metal oxide nanocrystals for chemical sensors. Proceedings of SPIE, 2015, , .	0.8	Ο
800	A Perspective: Could Carbon Current Collectors Improve the Energy Density of Aqueous Alkaline Symmetric Supercapacitors?. Energy Harvesting and Systems, 2016, 3, 287-296.	1.7	0
801	Introducing Professor J R Morante as Editor in Chief of Journal of Physics D: Applied Physics. Journal Physics D: Applied Physics, 2017, 50, 030201.	1.3	Ο
802	\hat{I}^2 -SiC on SiO2 Formed by ION Implantation and Bonding for Micromechanics Applications. , 2000, , 121-126.		0
803	Optical Spectroscopy of SOI Materials. , 2000, , 137-148.		Ο
804	SÃntesis por implantación iónica de nanocristales semiconductores para dispositivos en tecnologÃa de Si. Boletin De La Sociedad Espanola De Ceramica Y Vidrio, 2000, 39, 458-462.	0.9	0
805	Study of the Catalytic Additive Effects on the Properties of In ₂ O ₃ Nanopowders for Gas Sensing Applications. , 2003, , .		Ο
806	Processes for obtaining TiO2 anatase phase and their effects on the gas sensor performances. , 2003, , .		0
807	Estudio de la reacción de sulfurización de precursores Cu/In para la formación de capas delgadas policristalinas de CuInS ₂ para células solares. Boletin De La Sociedad Espanola De Ceramica Y Vidrio, 2004, 43, 348-351.	0.9	Ο
808	Estudio de puertas catalÃŧicas en sensores de gas en tecnologÃa de SiC. Boletin De La Sociedad Espanola De Ceramica Y Vidrio, 2004, 43, 383-385.	0.9	0
809	Construction and Test of a Multisensor Device Including a High-Sensitivity NO ₂ Sensing Module. Sensor Letters, 2008, 6, 1045-1048.	0.4	0
810	Synthesis and Sensing Properties of SnO ₂ Thin Films Obtained by Condensed Vapors Deposition. Sensor Letters, 2011, 9, 1282-1291.	0.4	0

#	Article	IF	CITATIONS
811	Control of the Si3N4-InGaAs Interfaces by Constant Capacitance Transients. , 1989, , 186-189.		0
812	A novel TEM technique for junction delineation in integrated circuits. Proceedings Annual Meeting Electron Microscopy Society of America, 1990, 48, 748-749.	0.0	0
813	Detailed analysis of \hat{I}^2 -SiC formation by high dose carbon ion implantation in silicon. , 1996, , 282-285.		0
814	Ion beam assisted recrystallization of SiC/Si structures. , 1996, , 334-337.		0
815	Stress gradient and structural properties of atmospheric and reduced pressure deposited polysilicon layers for micromechanical sensors. , 1996, , 9-12.		0
816	Coexistence of the CuPt type ordering and the fine contrast modulation in InGaP/GaAs layers depending on the substrate misorientation. , 2017, , 381-384.		0
817	On the lateral decomposition, growth mode and defect nucleation in the InxGa1-xAs channel of HEMT devices depending on the growth temperature, well thickness and mismatch. , 2017, , 491-494.		0
818	Modelling and HRTEM computer simulation of facetting of SnO2 nanostructures deposited by spray pyrolysis on glass substrates. , 2018, , 79-82.		0
819	HI.1 - Fully Integrated Electrochemical Sensors: a Disruptive Alternative Compatible With Microelectronics Procedures. , 2018, , .		0
820	Effects of in-situ and ex-situ reduction of Pd/SnO2 studied by HRTEM. , 2018, , 73-76.		0
821	High resolution electron microscopy analysis of Pt-nanoparticles embedded on crystalline TiO2. , 2018, , 69-72.		0
822	Noble metal distribution in mesoporous silica as a selective active filter for semiconductor gas sensors. , 2018, , 433-436.		0
823	Bi-Metallic Sn-Pd Catalysts for CO2 Electroreduction to Formic Acid: Modulation of Overpotential and Stability. , 0, , .		0
824	Integration of Adapted Thin-film Photovoltaics into Solar Vanadium Redox Flow Batteries for Energy Storage. , 0, , .		0
825	Scalable Production of Syngas from Solar CO2 Recycling. , 0, , .		0
826	Bottom-up Engineering of Hematite Nanowire Heterostructures for Photoelectrochemical Water Splitting. , 0, , .		0
827	Molecular Layer Deposition of Titanicone over Lithium Silicide Anode. ECS Meeting Abstracts, 2020, MA2020-01, 384-384.	0.0	0
828	Nanocontacts fabricated by focused ion beam: characterisation and application to nanometre-sized materials. , 0, , 291-294.		0

#	Article	IF	CITATIONS
829	Mesoporous Indium Oxide for Gas Sensor Applications. NATO Science for Peace and Security Series C: Environmental Security, 2009, , 67-75.	0.1	0
830	GaAs NWs and Related Quantum Heterostructures Grown by Ga-Assisted Molecular Beam Epitaxy: Structural and Analytical Characterization. , 2008, , 295-296.		0
831	Generation of Ammonia by High Concentrated Nitrate Electrolyte Electroreduction. , 0, , .		0
832	Integration of Adapted Thin-film Photovoltaics into Solar Vanadium Redox Flow Batteries for Energy Storage. , 0, , .		0
833	Scalable Production of Syngas from Solar CO2 Recycling. , 0, , .		0
834	Bi-Metallic Sn-Pd Catalysts for CO2 Electroreduction to Formic Acid: Modulation of Overpotential and Stability. , 0, , .		0
835	Bottom-up Engineering of Hematite Nanowire Heterostructures for Photoelectrochemical Water Splitting. , 0, , .		0
836	High Performance Lithium Silicide Electrode Enable By Molecular Layer Deposition. ECS Meeting Abstracts, 2020, MA2020-02, 1693-1693.	0.0	0
837	A Novel Î-D Conjugated Cobalt Tetraaza[14]Annulene Organic Framework for Efficient Electrocatalytic Co2 Reduction. SSRN Electronic Journal, 0, , .	0.4	0
838	Nanowires as Building Blocks of New Devices: Present State and Prospects. Ceramic Engineering and Science Proceedings, 0, , 1-8.	0.1	0